Accepted Manuscript

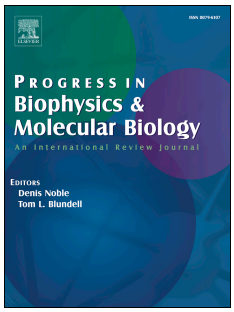

Biomechanical property and modelling of venous wall

Wenguang Li

PII: S0079-6107(17)30215-8

DOI: 10.1016/j.pbiomolbio.2017.11.004

Reference: JPBM 1298

To appear in: *Progress in Biophysics and Molecular Biology*

Received Date: 14 September 2017

Revised Date: 13 November 2017

Accepted Date: 15 November 2017

Please cite this article as: Li, W., Biomechanical property and modelling of venous wall, *Progress in Biophysics and Molecular Biology* (2017), doi: 10.1016/j.pbiomolbio.2017.11.004.

Biomechanical Property and Modelling of Venous Wall

Wenguang Li

School of Mathematics and Statistics
The University of Glasgow, Glasgow, G12 8QW, UK
Wenguang.Li@glasgow.ac.uk

18/11/2017

Abstract

Human saphenous vein has long been used as coronary artery bypass grafts to survive a heart arrested by blocked coronary arteries. Biomechanical properties of the saphenous vein can be critical because mismatch in the biomechanical property between a coronary artery and a graft will reduce graft patency and speed up disease development in the graft. In this paper hence the active and passive biomechanical behaviours of the human saphenous vein and other venous walls were reviewed extensively and comprehensively. The existing *in vitro* uniaxial, bulge, planar and tubular biaxial tensile testing methods, *in vivo* testing cases, property variables, various tested results, constitutive models and their mathematical modelling methods, viscoelasticity, and residual strain/stress are highlighted and summarized. It is demonstrated that the biomechanical properties of the human saphenous vein and other venous walls are not well documented, and their modelling approaches are limited and subjected to be updated in a great deal. Additionally, a few important research issues are proposed. The paper has provided a piece of useful information to investigation into coronary artery bypass grafts.

Keywords: saphenous vein; uniaxial tensile test; tubular biaxial inflation test; coronary artery bypass graft; residual strain; constitutive law

1 Introduction

Coronary artery disease (CAD) is an important cause of mortality all over the world. Human great saphenous vein (GSV) frequently serves as coronary artery bypass graft (CABG) to treat CAD because it easily is harvested and handled and without allograft rejection. Even though this idea can be traced back to 1930's [1], the direct coronary artery surgery by using CABG technique began actually in 1968 in the USA [2]. Currently, nearly 20,000 CABGs are carried out every year by NHS mainly to treat old people with age of at least 60years in England [3].

The GSV is a large, subcutaneous, superficial vein of the human leg. The vein runs along the length of the lower limb, as shown in Fig. 1(a). A segment of GSV can be cut off and used to bridge the blocked coronary artery and the aorta and form a bypass duct, see Fig. (b), eventually the blood can flow into the coronary artery to make the heart working properly.

Unfortunately, saphenous vein CABG has to experience an arterialization process after the surgery. In the process saphenous vein CABG can be failure and subsequent remodelling as well as develop various diseases such as aneurysms, thrombosis, atherosclerosis and fibro-intimal hyperplasia [6-10] which are associated with smooth muscle cells and extracellular matrix. In the first post-surgery month, 13-14% of grafts occlude because of thrombosis. By the end of the first year of the surgery, intimal hyperplasia develops to reduce graft diameter by 25-30%. In the following years, grafts occlude at a rate of 2% per year as intimal hyperplasia develops. Beyond 5years, vein grafts are in atherosclerosis due to necrosis, haemorrhage, calcification and thrombosis [10].

The failure and disease are closely linked to CABG physiological hemodynamic conditions [11] and GSV itself mechanical property such as compliance [12]. Up to now, a significant amount of review papers have appeared to clarify the problems in pathology, surgery and hemodynamic factors associated with saphenous vein CABGs, such as [6-11], just to name a few.

Additionally, there are a few review papers on artificial vascular grafts. The textile structures used in the construction of artificial vascular grafts were reviewed in detail and the structural factors relating to the failure of vascular grafts were identified [13]. The material properties and methods for determining the attributes of these factors to the failure are emphasized for further research. The mechanical mismatch of the artificial small-diameter vascular graft to the host vessel was reviewed and discussed [14]. It was pointed out that detailed characteristics, like anastomic behaviour, longitudinal elasticity, and flow-related variables should be taken seriously. Mismatch in compliance and diameter at the end-to-end anastomosis of a compliant artery and rigid artificial graft was reviewed comprehensively because the mismatch could result in shear rate disturbances to induce intimal hyperplasia and ultimately graft failure [15]. How mechanical properties, for example compliance mismatch, diameter mismatch, Young's modulus and impedance phase angle influence graft failure owning to intimal hyperplasia was discussed. The principal strategy was proposed to prevent intimal hyperplasia based on the design and fabrication of compliant synthetic or innovative

tissue-engineered grafts with viscoelastic properties similar to those of the human artery. A broad overview of the current state of prosthetic bypass grafts was conducted [16] and it was shown that prosthetic materials were most commonly used in high pressure, large flow conditions, such as the aorta and femoral arteries, but had not been as successful in other regions like carotid and coronary artery bypass surgeries. A new generation of polymers like polyurethanes should be used promptly.

A literature survey made by us with PubMed showed that a little attention has been paid upon biomechanical properties of GSV since 1960's. In consequence, there has not been such a paper to review the biomechanical properties of venous walls with an emphasis on GSVs so far. In this contribution, an attempt is made to summarize and interpret existing experimental and analytical results of the biomechanical properties and modelling methods of native venous walls. At first, the histology of venous wall is described briefly; then biomechanical properties of venous wall, including active tension, passive biomechanical properties are demonstrated and discussed; thirdly the methods for modelling the passive biomechanical properties are highlighted and summarized; finally need for further research and conclusions are drawn. The paper can be meaningful for biomechanical property identification, design of CABG, and biomechanical property modelling of veins.

2 Histology of venous wall

In average, the human vein is with 5mm diameter and 0.5mm thickness compared with the artery in 4mm diameter and 1mm thickness [17]. A healthy human saphenous vein wall consisted of three layers, namely intima, media and adventitia from inner to outer surface of the wall [18-21]. Generally, the intima was thin as 60.07μm±1.12, composed of endothelium and an internal elastic lamina next to the media. The media mean thickness was 360.54μm±4.56, in which there were longitudinally oriented and smooth muscle cells next to the intima and circular smooth muscle cells next to the adventitia, the two smooth muscle layers were separated by a collagen fibres. The adventitia was full of collagen fibres with some fibroblasts and capillaries as well as longitudinally oriented smooth muscle cells [21].

A detailed image of layer structure of blood vessel in the transverse section [17] is illustrated in Fig. 2. The intima is separated from the media by a thick elastic lamina. The intima is composed of single layer endothelial cells. The adventitia is separated from the media by another thick elastic lamina. The adventitia consists of dense collagen fibres, a few fibroblastic cells, occasional elastic fibres and vasa vasorum. The media has alternating layers of smooth muscle cell, elastin and collagen. Collagen appears to be blended with the elastin fibres. The smooth muscle cells connect with each other forming circumferential bundles. The smooth muscle cells link with the collagen and elastin fibres in parallel, which is consistent with the observation in [22]. Proteoglycans (PG) are the densest in the media than in intima and adventitia.

Presently, there is little information about collagen fibre orientation and dispersion in the human saphenous vein. A mean fibre orientation of 37 ± 6^{o} against the circumferential direction in the

media [23] in comparison with 40^o in porcine vascular tissues (including vena cava, abdominal aorta and iliac artery) was observed [17]. In the adventitia of the porcine vascular tissues, the fibre mean orientation was 60^o from the circumferential direction [17], see Fig. 3.

Collagen fibres were wavy at zero-load, and then they became straight with increasing load [24]; this is so-called fibre recruitment mechanism for the engagement of tension. Waviness index (WI) and its probability density distribution are of vital importance for describing the recruitment mechanism of fibres. WI was defined as the ratio of the length of an elastin lamella to the straight line distance between two reference points [24]. In the rabbit aortic media, WI decreased to 1.05 at 80mmHg transluminal pressure or more from 1.65 at zero pressure [24].

For the rabbit descending thoracic aorta, left common carotid artery (between its origin and carotid bifurcation), inferior vena cava (thoracic segment), and external jugular (on the same side and height as the carotid artery), the WIs of elastin in media and adventitia and the WI of collagen in media were measured optically at zero-load state [25]. It was found that WI of collagen was 1.2 in the aorta and carotid artery, but 1.57 in the inferior vena cava and jugular vein. WI of elastin in media and adventitia showed a little difference, it was 1.1 in the aorta and carotid artery, but increased to 1.42 in the inferior vena cava and jugular vein.

The orientation and WI of collagen fibres in media and adventitia of the human inferior vena cava were measured optically [26]. The collagen fibres were distributed circumferentially in the media but longitudinally in the adventitia. The mean WI of collagen fibres was 1.24 compared with 1.57 in the rabbit jugular vein [25] and 1.25 in the rabbit carotid artery adventitia [27]. Further, the WI stochastic distribution in the media adventitia could be best fitted by using Weibull, Gama and Beta probability density distributions, respectively.

The dry weight contents of collagen, elastin and smooth muscle in walls of the man aorta and femoral vein, saphenous vein were measured chemically [28], and the femoral vein is subject to a double high collagen content and one third elastin content as well as 5% less smooth muscle content in comparison with the aortic wall, see Fig. 4(a). In the wall of the super segment of saphenous veins, the contents of collagen, elastin and smooth muscle are basically identical to the femoral vein for the subjects at different ages, as shown in Fig. 4(b).

Recently, volume fractions of collagen and elastin were measured in the porcine aorta, carotid, iliac and vena cava, are shown in Table 1 [17]. The total collagen volume fraction in the vena cava is higher than those in aorta, carotid and iliac artery, but the elastin in the vena cava seems to close to the aorta and less than carotid iliac artery. In media, the content of collagen is less than those in aorta, carotid and iliac artery. The content of collagen in the adventitia is higher than in the adventitia of aorta, carotid and iliac artery. Thus, the vein will be more compliant at a small strain, but stiffer at a large strain.

For the rabbit descending thoracic aorta, left common carotid artery, inferior vena cava, and external jugular vein, the area fractions of collagen, elastin and smooth muscle in them were measured

[25] and listed in Table 2. Clearly, the venous walls are subject to higher collagen content but lower elastin and smooth muscle contents compared with the arteries.

The contents of collagen I, III and IV and elastin in the human femoral vein (FV), incompetent saphenous vein (ISV) and competent saphenous vein (CSV) were measured by using computer-image-analysis system connected to a microscope based on immunohistochemically staining technique in terms of area fraction occupied by collagen or elastin in transverse sections [29]. The area fractions of these vein samples are tabulated in Table 3. ISV is subject to the highest elastin content and the least compliance in comparison with CSV.

Note that collagen content in healthy venous walls is different from diseased venous walls. For example, the long saphenous vein was subject to a low level of collagen content than in varicose veins [30, 31].

3 Biomechanical properties of venous wall

Like the biomechanical properties of arterial tissue, the biomechanical properties of venous wall consist of active behaviour and passive characteristics. The active behaviour is associated with the contraction of smooth muscle cells in the wall under a stimulus. The contraction can induce the other tissue components such as elastin and collagen fibres are in tension to raise the transmural/transluminal pressure level. The passive characteristics of venous wall stand for the hyperelasticity and viscoelasticity of the wall under a transmural pressure and at an axial stretch when a stimulus is absent.

3.1 Active biomechanical property

Because venous wall has smooth muscle, it naturally can generate contracting tension. Usually, the active contracting behaviour of venous wall is characterized *in vitro* by means of mechanical or electrical or chemical stimuli on a strip harvested from a venous wall under isometric or isotonic conditions. Until 1960's, observations on the active contracting are not quantitative basically. For example, a very early observation on active contraction of venous wall was made in 1902 [32]. Arteries from 35 oxen and a considerable number of horses, cats and men were examined with various stimulators such as freezing, heating, bathing of olive oil and so on. Like arteries, jugular vein could respond to stimuli generated by these stimulators, exhibiting an active contraction.

Helically cut strips of the cat portal vein were stretched isotonically with and without norepinephrine, epinephrine, isoproterenol, K ion and so on, it was confirmed that these chemicals could induce venous smooth muscle to contract [33]. The same experimental method was applied into helically cut strips of the cat portal vein as well [34], it was identified that the intracellular concentration level of calcium ion exhibited a key effect on determining resistance of smooth muscle to stretch. In [35], the contractile properties of spiral strips and isolated segments of the lateral saphenous vein of the dog were studied with electrical stimulation. Stimulation could make length-

load or pressure-volume curves stiffer, and the active tension first increased with progressive stretch, but it reduced when the specimens were overstretched. In [36], strips of the dog saphenous vein were examined and it was found that they could contract during warming (43^oC) and relaxed a little during cooling (to 29^oC). Spontaneous rhythmic contractions were observed in a few preparations of the human isolated saphenous veins from old subjects (>60 years) [37]. These experimental facts suggested that contraction of saphenous veins was related to intracellular Ca^{2+} signalling which was involved smooth muscle [38-40], and might be modelled by using methods proposed in [41-43]. However, there has been no investigation into active contraction of saphenous vein so far.

Adaptation of active contraction of saphenous vein along with smooth muscle cell orientation in arterial circulation after CABG surgery is another key important issue. In [44], a segment of the canine saphenous vein was used as arterial graft, and its thickness and content of all measured proteins increased but the maximum contractile response decreased. Additionally, the response characteristics of saphenous vein grafts to various medicines in arterial flow condition have been clarified by a number of researchers [45-50]. However, theses interesting outcomes are belong to biochemical subjects and out of the scope of this paper, thus have to be omitted here.

3.2 Passive biomechanical property

Passive biomechanical property of venous wall is composed of two properties, namely hyperelasticity and viscoelasticity. The hyperelasticity can be achieved by preconditioning *in vitro* only and is independent of stain rate, and eventually can be described by a constitutive law. Such a law can be presented by capacity or compliance, pressure-diameter/radius relationship, incremental Young's modulus, stress-stretch/strain relationship and strain energy function etc., depending on the level of our understanding of the subject and our interests. The viscoelasticity is a passive property of a venous wall *in vivo* or *in vitro* without preconditioning. This property cannot be represented by a constitutive law for hyperelasticity alone; instead both strain rate and time-history effects should be considered together.

3.2.1 The hyperelasticity property

Usually, the hyperelasticity property of venous wall is characterized experimentally *in vitro*. The experimental methods include tubular simple inflation test, biaxial inflation test, and uniaxial simple/tensile test as well biaxial tensile test. The tubular simple inflation test started in 1960's. In the experiment, a blood vessel segment was isolated from the organ, the one end of the segment was closed and the other end was connected to a tube. The segment was immerged in the saline in a basin and inflated with a positive pressured fluid through the tube, and only the diameter of the segment was recoded manually at each experimental transluminal pressure. A typical tubular simple inflation experimental apparatus can be found in [51]. Based this method, compliance, pressure-diameter/radius relationship, global and incremental Young's moduli of a venous wall can be obtained.

It was worthy of mentioning that an apparatus was designed to measure dynamic compliance of blood vessel by using a sensor, i.e. a miniature elastic cantilever beam *in vivo* [52].

As an updated version of tubular simple inflation experiment, in the latter of 1960's, a few biaxial inflation approaches, namely bulge method [53, 54] and vessel segment inflation method [55-58], were designed to identify the biaxial biomechanical properties of the vessel. In the bulge method, a flat piece of a vessel was fixed between two plates, which had a circular hole and were mounted on a rigid container. The container was inflated with a positive pressure and the flat piece forms a dome-shaped bulge. The dome was approximated by a part of a sphere and the tension or the Cauchy stress was calculated from the Young-Laplace's law for sphere. The radius of the sphere could be determined with optically measured displacements of the markers on the dome surface [53], or estimated with the instant liquid volume delivered by the infusion pump and the measured apex height as well as the radius of the hole [54].

In principle, if the sphere approximation is held, the bulge method is applicable for isotropic elastic materials *in vitro* only. Recently, the method has been utilized to identify anisotropic soft tissue by employing both a high resolution approach for measuring strain field and a complicated numerical method for dealing with mechanics model to extract biomechanical properties [59, 60].

During vessel segment inflation tests [55-58], both the diameter and the length of the segment were recoded simultaneously, the tests could capture the biaxial deformation feature in the vessel. In the vessel segment inflation method of [55], the segment was in dry air, however, in the segment inflation method of [56-58], the specimen was immerged horizontally in a liquid basin to make experimental temperature controllable.

Vessel segment inflation tests are subject to a few limitations, namely complex equipment, tedious testing procedure and being difficult to capture the break/fracture behaviour of soft tissue. Hence, since 1970's uniaxial simple/tensile testing method has emerged. In the method, one specimen is a ring cut from a vessel and is used to show the mechanical property in the circumferential direction, the other specimen is a segment [61] or a strip sample [62-64] harvested from the vessel longitudinally. Then two specimens are stretched on a material testing machine, respectively.

In uniaxial tensile tests, the soft tissue is stretched in the loading direction only, in the two transverse directions, however, the tissue is compressed, and in consequence the fibres in the tissue are compressed in these directions as well. In order to break the specimen, the tissue must undergo a significant large stretch to achieve the fibre ultimate strength or stretch. Usually, the stretch applied is much larger than the stretch in a soft tissue under physiological conditions.

To remove the limitation of uniaxial tensile test, planar biaxial testing method occurred in 1970's. In the test, a soft tissue specimen is in squared-shape, and is stretched in two orthogonal directions with a certain transverse extension ratio, which is the ratio of the extension in the primary direction to the extension in the transverse direction when two loadings are applied during an experiment [65, 66]. Since the tissue is stretched in both directions, the fibres in the tissue are always

in tension and can reach their ultimate stretch or strength very quickly with increasing two stretches applied. In fact, we don't exactly know what the extension ratio is when a soft tissue works under physiological conditions. Therefore, the soft tissue has to be tested under various transverse extension ratios. Obviously, how to specify the ratio in a biaxial tensile test for mechanical property constants determination is an issue of test protocol [67, 68], because the mechanical property constants depend on the transverse extension ratios [68].

Vessel segment inflation test mentioned above is tubular biaxial tensile test. An interesting comparison of two typical biaxial testing methods was made [69] by using the porcine coronary arteries. The mechanical property constants were determined based on planar biaxial tests firstly, then applied them into the porcine coronary arteries at 0-120mmHg intraluminal pressures. It was turned out there was a 12.3% error in pressure-diameter relation against the inflation test and the difference in circumferential stress could be as high as 50.4% between the model and the measurements.

By making use of the experimental methods above, a few important characters of venous walls, such as compliance, pressure-diameter/radius relationship, global and incremental Young's moduli and stress-strain curve of a venous wall, have been measured and interpreted extensively in literature. Here just a brief summary is delineated and highlighted.

1) Compliance

Compliance of a pressurized organ is defined as a volume change with respect to intraluminal pressure change, i.e.

$$C = \Delta V / V \Delta p \times 100\% \tag{1}$$

where V is the initial volume of the organ, Δp is the pressure change, and ΔV is the change in volume induced by Δp [52]. For a cylinder model of the organ, the compliance can be simplified to the following expression

$$C = \Delta D / D \Delta p \times 100\% \tag{1a}$$

where D is the initial diameter of a vessel segment and ΔD is the change in diameter induced by Δp. In [51], however, the compliance was called volume distensibility coefficient. The reciprocal of the compliance was considered the Young's modulus of an organ segment [70]. The compliance represents a global biomechanical behaviour of an organ simply and roughly, and has been applied in clinical practice extensively. The compliance includes static value [51] and dynamic value that related to the heart systolic and diastolic states [52] and can be measured *in vitro* [52, 71] and *in vivo* [72].

Compliance mismatch between saphenous vein graft and artery can degrade the graft performance and result in a loss of patency, which is the degree of openness of a vessel, in term of time after surgery [73]. The compliance of eight human femoral arteries, five types of arterial grafts such as human GSV, Glutaraldehyde-treated human umbilical cord veins, modified bovine heterograft, velour Dacron and expanded polytetrafluoroethylene were measured by inflating the segments of

these conduits on a device [74]. The compliances of the human GSV, Glutaraldehyde-treated human umbilical cord veins were 3/4 and 2/3 of the compliance of the human femoral artery, respectively. The compliance of the rest grafts was half below the compliance of the artery. Experiments were performed on a low flow canine femoral artery bypass models of femoral vein, double velour Dacron and expanded polytetrafluoroethylene (ePTFE) [75]. The compliances of dissected artery, femoral vein, double velour Dacron and PTFE were 0.074, 0.027, 0.019 and 0.016%/mmHg, respectively. It was identified that the larger the compliance was, the higher the patency was. Similarly, the compliances of poly (carbonate) polyurethane (CPU) vascular graft, artery, ePTFE, Dacron and human saphenous vein were measured under the pulsatile flow condition of a phantom *in vitro* [76], It was shown that CPU and artery were subject to 0.081 and 0.080%/mmHg mean compliances, but ePTFE and Dacron were with mean compliances as low as 0.018 and 0.012%/mmHg, respectively. The human saphenous vein had a similar mean compliance at a lower pressure than 30mmHg, however, its mean compliance dropped significantly at a pressure of 30-50mmHg, and beyond 50mmHg, the compliance remained unchanged.

Like [15], the patency will present a linear relationship with the compliance, as shown in Fig. 5 if the experimental patency and compliance are plotted together for the host artery and various kinds of grafts one year after graft surgery. A comprehensive review on compliance and its measurement methods for vascular grafts has been made in [15], and they are no longer repeated here.

Based on the work in [77, 78], the diameters of GSV with and without nitroglycerine were examined by using ultrasound method *in vivo* in 12 elderly and 5 young healthy men after 6min venous stasis (up to 60mmHg cuff pressure) and the compliances of GSV were calculated [79]. It was indicated that GSV compliance in the elder group was higher than the younger group. Nitroglycerine could make GSV more compliant in both groups.

2) Pressure-diameter relationship

The internal diameter/radius-pressure relationship is one important response of saphenous veins or arterial grafts to a series of pressures *in vitro* or *in vivo*, and it can reflect the change of passive biomechanical behaviour during arterialization. It can be used as an index of passive biomechanical property of arterial grafts in clinical application potentially.

The pressure-diameter relationship of GSVs harvested from the human lower leg and upper legs was tested *in vitro* in [73]. The GSV vein segments of the upper leg were softer than those of the lower leg if the pressure was lower than 50mmHg, beyond that pressure two groups share nearly the same pressure-diameter relationship.

The external jugular veins and femoral veins were obtained from adult cats and their volume-pressure relationship was measured *in vitro* [80]. Subsequently, the volume-pressure relations of healthy human GSVs and the GSVs from patients with varicose veins were tested *in vitro*, and it was

clarified that the GSVs from patients with primary varicose veins exhibited larger radii and were more distensible than the healthy GSVs [81].

Passive biomechanical and histological properties of dog femoral veins were investigated after their implantation as grafts to bypass the ligated femoral arteries [82]. The internal diameter of the grafts increased quickly in 4weeks after implantation. Intimal hyperplasia and medial thickening were observed in response to high blood velocity and pressure in the arterial physiological condition.

Before CABG surgery, GSV segments need to be distended manually with liquid solutions to increase their patency. It was demonstrated that a pressure between 150-300mmHg could result in medial damage [83].

The saphenous vein grafts can be implanted in situ or reversely. The effects of these two techniques were examined by measuring the elastic properties of newly implanted grafts with vessel wall Doppler tracking method [84]. The diameter and pulse pressure were recorded, and relative distension, distensibility coefficient and compliance were calculated. The elastic properties of newly implanted grafts were comparable with native artery. Compliance mismatch was found around the proximal anastomoses of the grafts reversely implanted in comparison with the graft implanted in situ.

The diameter-pressure relationship of GSVs harvested from the human lower leg and upper leg was tested *in vitro* [85]. The internal pressure in these samples was increased up to 150cm H_2O stepwisely and the outer diameter was measured continuously with a video micrometre system in which a microscope was connected to a video camera and a monitor, the diameter was calculated by trigging dark-light transitions in the video signal. Eventually, compliance was calculated and plotted against the pressure. It was identified that the human lower leg and upper leg GSVs showed less difference either in diameter-pressure or compliance-pressure relationships, especially at a pressure more than 50cm H_2O.

An experimental set up was built, and 25-40mm long human saphenous vein segments were inflated with a pressure up to 100kPa and an axial load ranging up to 100N. The surface deformation was tracked by tracing twelve markers in 3D space using 2 CCD cameras. Results showed that the deformation of the vein was not axis-symmetric. The loading and unloading paths were not different, and the vein was compressible [86].

3) Global and incremental Young's moduli

Global Young's modulus or volume stiffness is the reciprocal of the compliance, C, mathematically [70], i.e.

$$E_p = V\Delta p/\Delta V \tag{2}$$

or the pressure strain elastic modulus or elastance [52]

$$E_p = D\Delta p/\Delta D \tag{2a}$$

Like compliance, the global Young's modulus stands for the stiffness of an organ as a whole only. The elastance of normal artery, autogenous vein graft of the dog, Dacron graft and synthetic graft material-modified human umbilical cord vein with a polyester mesh covering (DBM) were measured dynamically with a mean pressure 133mmHg *in vitro* initially, then the elastances at implantation and after the implantation for 2weeks were measured [52] and illustrated in Fig. 6. Theses graft materials seem stiffer than the host arterial wall and become softer after implantation.

The elasticity of the human vein segments harvested from autopsy material was measured in terms of global Young's modulus in five age groups such as 10-14, 20-30, 30-40, 40-50 and 50-70years by using *in vitro* vessel segment inflation experiment when the transmural pressure was in a range of 20-60mmHg, and a few *in vivo* experiments were conducted, too [70]. The global Young's modulus varied significantly in terms of subject age and decreased consistently with increasing age.

The incremental Young's modulus is defined as the ratio of an incremental stress to the incremental strain caused from the incremental stress at a strain

$$E = \Delta\sigma/\Delta\varepsilon \tag{3}$$

where $\Delta\sigma$ is the incremental stress, and $\Delta\varepsilon$ is the incremental strain due to $\Delta\sigma$. This is a quasi-linear method to characterize a nonlinear stress-strain curve. Naturally, the incremental Young's modulus is dependent on strain itself.

Dog pericardium and cat mesentery were measured using the bulge method and the Cauchy stress-stretch curves were fitted by using the stress-stretch relation for rubbers [53]. The incremental Young's moduli and compliances of canine femoral and jugular vein segments were studied with the bulge method as well [54]. The compliances of the femoral and jugular veins were lower than those of the carotid artery by nearly half at an intraluminal pressure higher than 40mmHg; accordingly, their incremental Young's moduli were larger than the artery.

A bulge inflation device was designed and used to measure the samples of 11 patients' human saphenous vein. The bulged surface was monitored with a microscopic camera; the deformed shape was best fitted in finite element analysis (FEA) simulations of ADINA 8.8 software by assuming the Young's modulus on a trial-and-error basis by employing on the linear homogenous elastic model at a pressure such as 22, 25, 31, 37, 43, 49, 60, 72 and 84kPa [87]. The Young's moduli determined showed a rising trend with increasing internal pressure.

The vessel segment inflation method was used to study incremental Young's moduli of dog and man venous walls [55]. A 5-10cm segment of vein was isolated and its length and diameter were measured *in vivo*, finally dissected from a subject. Special supporting plugs were inserted into the lumen. The superior plug was with a needle to allow a pressured normal saline with 5% dextrose to be pumped into the lumen. The segment was suspended vertically from its superior plug and the *in vivo* length was restored by using a small weigh of 5g hung on the other plug. The length and diameter of the segment were monitored with a 35mm camera and in experiments when the pressure was in a

range of 0-200cm H_2O with longitudinal forces ranging 0-20g. Based on the homogeneous, thin-walled, cylindrical vessel segment membrane model, i.e. stresses are uniform across the wall thickness [88], three Cauchy stress components at an intraluminal pressure, p, and a longitudinal force, F, are estimated by using the following equations

$$\begin{cases} \sigma_\theta = p\left(r/h - 1/2\right) = p\left(\lambda_\theta r_0/\lambda_r h_0 - 1/2\right) \\ \sigma_z = \frac{p}{2}\left(r/h - 1/2\right) + F/2\pi rh = \frac{p}{2}\left(\lambda_\theta r_0/\lambda_r h_0 - 1/2\right) + F/2\pi\lambda_\theta r_0 \lambda_r h_0 \\ \sigma_r = -\frac{p}{2} \end{cases} \tag{4}$$

where σ_θ, σ_z and σ_r stand for the stresses in the circumferential, longitudinal and radial directions, respectively, and r is the mid-wall radius, $r = \lambda_\theta r_0$, r_0 is the un-deformed mid-wall radius and λ_θ is the circumferential stretch, the longitudinal stretch, $\lambda_z = l/l_0$, l is the segment length at a p and F, l_0 is the un-deformed length, based on the assumption of incompressibility of tissue, $\lambda_\theta\lambda_z\lambda_r = 1$, the radial stretch is calculated by $\lambda_r = 1/\lambda_\theta\lambda_z$, h_0 is the un-deformed wall thickness.

Once having the stress values, two incremental Young's moduli can be calculated by the following expressions [55]

$$\begin{cases} E_\theta = \left(1-\nu^2\right)\dfrac{\Delta\sigma_\theta}{\Delta\lambda_\theta/\lambda_\theta} \\ E_z = \left(1-\nu^2\right)\dfrac{\Delta\sigma_z}{\Delta\lambda_z/\lambda_z} \end{cases} \tag{5}$$

where ν is the Poisson ratio, and ν=0.5 for incompressible tissues. Two Young's moduli in Eq. (5) are determined under λ_z=constant and λ_θ=constant conditions, respectively. Note that a general method for calculating incremental Young's moduli in variable λ_z and λ_θ circumferences was developed in [58], because of its linear infinite strain assumption, unfortunately, the method is no longer popular presently.

According to the vessel segment inflation method above, the relationships between radius and intraluminal pressure, incremental/tangential Young's modulus and intraluminal pressure of dog vena cava, jugular vein were presented and compared with those of pulmonary artery, descending aorta and carotid artery [55]. It was identified that the veins were much less flexible than the arteries, i.e. at the same intraluminal pressure level the radius of veins was smaller than the arteries. Accordingly, the circumferential incremental/tangential Young's modulus of the veins was much higher than the arteries, for instance, at 50cm H_2O (36.8mmHg) column height, the former was 4000kP, but the latter was 100kPa only.

The author of [89] illustrated and interpreted his *in vitro* vessel segment inflation experimental results simply, especially the incremental circumferential Young's modulus, on the dog vena cava, jugular vein, pulmonary artery, descending aorta and carotid artery. In the range of 0-100cm H_2O pressure, the Young's moduli of two veins were higher than the arteries.

4) Stress-stretch curves

The vena cava superior, and the intrathoracic and abdominal portions of vena cava inferior excised from dogs and their stress-strain curves were measured [90]. The circumferential and longitudinal stresses, σ_c and σ_l, were fitted by the exponential functions of the circumferential and longitudinal strains, ε_c and ε_l, independently.

About fifty 3mm samples were cut circumferentially from segments of the human long saphenous vein at the thigh, near knee and near the ankle for normal and varicose veins and stretched on a material testing machine under moist conditions [30]. The breaking strength was obtained, and the normal veins were with 970kPa mean breaking strength compared with 490kPa breaking strength for varicose veins. At the thigh, knee and ankle, the mean breaking strengths were 1100(710), 740(48) and 50(30)kPa for the normal (varicose) veins.

Human saphenous and umbilical veins were obtained from patients after their CABG surgery. The longitudinal specimens and circumferential rings from the veins were measured by simple tension test, respectively [64]. The circumferential and longitudinal stress-stretch curves were fitted with a 4^{th}-order polynomial and the maximum stress and stretch were analysed. Typical stress-stretch curves of four pairs of the human saphenous vein specimens and three pairs of the human umbilical vein samples are illustrated in Fig. 7. Both the veins are stiffer in the longitudinal direction than in the circumferential direction.

Saphenous vein segments (45 samples circumferentially, and 38 longitudinally) were harvested from 22 patients in whom there was excess vein after CABG surgery [91]. The longitudinal samples were in 40mm length, and the circumferential simples were 5mm wide rings. Both were stretched in the uniaxial direction in a servo-hydraulic material test system along with videocassette camera. A series of parameters, for example failure force, ultimate force, stiffness, failure stress, failure strain and modulus were decided. It was shown that the saphenous vein was stiffer in the longitudinal direction than in the circumferential direction.

Specimens of bovine jugular and lumbar veins harvested circumferentially and longitudinally and stretched using a custom-built saline bath in a MTS Tytron 250 material testing system [92], and results demonstrated the bovine veins were generally stiffer in the circumferential direction than in the longitudinal, as shown in Fig. 8, and the strain rate seemed to have little effect on the mechanical and failure property parameters of bovine veins, as has been observed in testing of other soft tissues.

Forty human saphenous vein samples were harvested after CABG surgery [93]. The planar biaxial tensile tests were conducted on the specimens from these samples. The stress-strain curves showed some degrees of anisotropy. The obtained stress-strain data were fitted with the anisotropic four-parameter Fung-type model and the five-parameter Mooney–Rivlin model. The tested data exhibited stiffer behaviour in the longitudinal direction in comparison with the circumferential

direction. The stretch in the circumferential direction was much higher than in the longitudinal orientation.

Excess segments of saphenous vein from the knee region were harvested from 15 patients that were subject to CABG surgery and measured by vessel segment inflation test in an organ bath [94], and the pressure-diameter relationship and stress-strain curves in both the circumferential and longitudinal directions were obtained. The stress-strain curve of the sample distended manually was stiffer than that without distension. Also, the longitudinal stress-stain curve was stiffer than the circumferential curve.

Saphenous vein segments were collected from 36 patients undergoing CABG surgery, and distended with a pressure in ranged 50-60, 75-100 and 130-150mmHg, and the ring-shaped samples were tested on a uniaxial material testing machine to get the circumferential stress-strain curves [95]. It was indicated that the curves was stiffer with increasing distending pressure and micro-fibrillary damage was observed at an even low distending pressure, namely in a range of 50-60mmHg.

The inferior vena cava from two models used in tissue engineering: wild-type C57BL/6 and immuno-deficient CB-17SCID/bg mice was measured by using vessel segment inflation method [96]. The circumferential and longitudinal stresses were fitted with the constitutive law of two-families of fibres in [97] and the law of four families of fibres in [98], respectively. Results demonstrated that inferior vena cava from the latter was considerably stiffer in the circumferential direction, both materially and structurally, even though there were a lower intramural content of collagen and similar wall thickness.

Three human GSV segments were inflated with an intraluminal pressure at 0.04, 0.5 and 1Hz loading rates, respectively [99], then the Cauchy stress-stretch curves were fitted with the constitutive law proposed by [97].

Human GSV segments were collected from patients after CABG surgery or autopsies with 24h after death, then a series vessel segment inflation tests were conducted to obtain the circumferential and longitudinal stretch curves in terms of intraluminal pressure [100]. The curves were fitted by using strain energy function of [97] with residual circumferential stretch. Since the fibre orientation dispersion was not taken into account, fitted curves were slightly poor against experimental data.

3.2.3 The viscoelastic properties of venous wall

Blood vessels with collagen fibres can exhibit viscoelastic behaviour under physiological conditions. The behaviour is apparently a time lag in response to a loading applied because of the friction between molecules in the material [101]. This behaviour manifests itself in three appearances, depending on loadings and strain conditions, such as hypothesis loop for cyclic loading, relaxation at a constant strain and creep at a constant loading. The viscoelasticity can be characterized by using *in vivo* vessel diameter dynamic observation [101-103] and *in vitro* uniaxial tensile tests, namely

incremental stress-strain test [62, 63], normal stress-strain test with cyclic loading [92, 105, 105], and ramp stress-relaxation experiment [106, 107].

The ramp stress-relaxation experiment is actually a uniaxial tensile test with a ramp strain initially and a subsequently constant strain held for an hour for specimen relaxation. The quasi-linear viscoelastic (QLV) or Fung's theory is often used to build the viscoelastic constitutive model of the specimen. In the QLV theory, the history of the stress response is separated into the nonlinear elastic response and a time-dependent reduced relaxation. The nonlinear elastic response obeys ordinary constitutive laws for soft tissue. The reduced relaxation function with three material parameters represents the time lag in a response. If the exponential function with two material parameters is chosen as the stress-strain relation of nonlinear elastic response, the QLV viscoelastic constitutive law is subject to five parameters, which can be optimized with Levenberg-Marquardt algorithm or genetic algorithm [108] by minimizing the error in the stress between model predictions and experimental values at a series of strains.

The stress-relaxation tests in specimens harvested from the human saphenous veins in the circumferential and longitudinal directions were done with 20% and 50% strains [109]. It was demonstrated that the saphenous vein had non-linear viscoelastic behaviour. The QLV constitutive model was fitted with stress relaxation curves and the five model parameters were determined. However, the stress relaxation equation in [109] seemed incorrect because there was no integral with respect to time history in the equation.

3.2.4 Residual strain in venous walls

There is residual strain in the wall of tubular structures such as blood vessel, left ventricle, trachea, ureter, oesophagus and gastrointestinal tract and so forth when the loading on the structure is zero [110]. The residual strain in a structure must result in a residual stress in the structure under zero loading condition.

To decide the residual strain, we need know the zero stress state of the structure by releasing the residual stress. For a blood vessel, a simply approach for showing the zero stress state is to cut the vessel into a number of ring segments transversely, subsequently, each ring is cut radially once, resulting in it to open. These opening structures, which are in the first order of infinitesimals in zero stress, are considered the zero stress state of each vessel segment [111].

After the lengths of a vessel segment inner and outer walls in the zero load and zero stress states are measured, respectively, the residual strain in the zero load state can be calculated straightaway. Note that the vessel zero sate structure likes a sector, thus an opening angle of the sector is used to characterize the structure feature. The opening angle is defined as the angle subtended between two radii with origin positioned at the midpoint of the inner wall and through the tips of the inner wall, see Fig. 9.

Usually, the opening angle of a blood vessel is larger than zero, suggesting its inner wall is compressed whilst its outer wall is in tension. As a result, the residual strain makes the circumferential stress distribution across the blood vessel wall more uniform than the case without residual strain, as shown in Fig. 10.

It is difficult to estimate the residual stress in a blood vessel based on a known residual strain. One method is bending vessel zero stress structure with a force step by step in an experiment until it is closed, then a beam mechanical model is established based on a homogenous linear stress-strain relationship or the well-known Fung's stress-strain exponential law, finally the mechanical property constants are determined inversely by minimizing the error in the displacements between measurement and model prediction with the modified Powell's hybrid algorithm [112]. Even though this method is applicable for a zero stress configuration in any shape, it requires extra experiments except the zero stress observations, and it is less in use at the moment.

The other method is thick-walled cylinder method which was proposed initially in [113]. In the method, the zero stress structure of a blood vessel is assumed to be a circular sector, the zero load configuration and loaded vessel all are cylindrical. Based on the incompressible condition, the geometrical relationship between the zero stress configuration and a deformed configuration can be established simply. If the zero load configuration and a series of stretch-pressure experimental data points have been available, then an inverse problem can be solved to obtain the biomechanical property constants in a constitutive law such as six-parameter Fung's model in [113] and three-parameter Guccine's model in [114]. Once these constants in the law are obtained, the residual stress can be calculated accordingly.

Like arteries, veins can be subject to residual strain, as shown see Fig. 11 for various veins of rat observed [115], in particular, the opening angle of the rat saphenous vein was as low as 25^o in average. For porcine, 115 and 120^o mean opening angles were found in the outflow cuff segment and the cerebral bridging vein [116]. Similarly, for the human, the mean opening angle of pulmonary veins was between 89 and 128^o in comparison with 92 and 163^o of the arteries [117].

For the human saphenous vein, the mean opening angle could be large as 120^o [99]. However, more recent observations illustrated that the opening angle was in a range of 34-57^o with a mean of 45^o for four patients aged 55(F), 60(F), 67(M) and 65(M) [118].

Opening angles of 30 canine autogenous vein grafts after surgery at 1day, 1week, 4 and 12weeks were measured and compared with the opening angle of canine femoral vein [119]. Results demonstrated that the mean opening angles of vein grafts were -0.4, 6.1, 25.4 and 47.8^o, respectively, at 1day, 1week, 4 and 12weeks in comparison with 63^o of the normal formal veins of the subject. The increasing opening angle after surgery was related to non-uniform transmural tissue remodelling process, especially the intimal hyperplasia or thickening effect.

4 The hyperelastic property modelling

As shown above, venous walls are an anisotropic, nonlinear elastic material. Even though incremental circumferential and longitudinal Young's moduli can be obtained separately and in uncoupled state, they are in coupling state in reality. Additionally, venous walls are with more content of collagen but less mass of elastin in comparison with arterial walls as presented in Tables 1 and 2 as well as Fig.4. As a result, the stress-strain curve of venous walls is more compliant than the curve of arterial walls at a low strain, but stiffer than that of arterial walls at a high strain. In order to model the hyperelastic biomechanical property of venous walls precisely, these two issues should be reflected in modelling methods. This is the difficulty in constitutive law modelling for venous walls.

There are three types of method for modelling the hyperelastic biomechanical property of venous walls, and summarized in Table 4. The first type is phenomenological method, in which one stress component is correlated to its corresponding strain component empirically and separately, or the coupling in the stress between the circumferential and longitudinal directions is handled with an empirical correlation. In the second type, however, the coupling is accomplished mathematically by a strain energy function based on a few strain/stretch invariants without the collagen fibre recruitment mechanism explicitly but with an exponential function implicitly. In the third type, the coupling is treated with a strain energy function with stochastic fibre recruitment mechanism.

4.1 Phenomenological methods

Two exponential functions of circumferential and longitudinal strains, ε_c and ε_l were proposed and applied to fit the circumferential and longitudinal stresses σ_c and σ_l, of the dog vena cava, separately [90]. These exponential functions are presented by the following expressions

$$\begin{cases} \sigma_c = c_1\left(e^{c_2\varepsilon_c}-1\right)+c_3\left(e^{c_4\varepsilon_c}-1\right) \\ \sigma_l = c_5\left(e^{c_6\varepsilon_l}-1\right) \end{cases} \tag{6}$$

where c_1 to c_6 are constants determined by a nonlinear least squares method. Since one stress component is related to the strain along this stress component direction only, the two stress expressions are uncoupled and independent of each other.

A piecewise expression was put forward to best fit experimental longitudinal stress-strain curves of the rabbit inferior vena cava and external jugular vein and to precisely take into account of the responses of elastin and collagen fibres in the venous walls [25]. The expression consists of a power function and an exponential function of longitudinal strain

$$\sigma_l = c_1\varepsilon_l^{c_2}+c_3\left(e^{c_4\varepsilon_l}-1\right) \tag{7}$$

where c_1 to c_4 are constants determined by a nonlinear least squares method against the experimental stress-strain data points.

In [120], 2D phenomenological constitutive law, called bedspring model, was put forward to model the experimental data of thin-walled cylindrical rat vena cava. It was found that the

experimental circumferential-to-longitudinal first Piola-Kirchoff stress ratio could be best fitted with an empirical hyperbolic correlation in terms of circumferential stretch with two constants as follows

$$f\left(\lambda_\theta\right) \equiv \frac{s_\theta}{s_z} = \frac{c_1}{\left(c_2 - \lambda_\theta\right)^2} \tag{8}$$

where s_θ, s_z are the first Piola-Kirchoff stresses in the circumferential and longitudinal directions, respectively, c_1 and c_2 are property constants. This correlation represents the coupling of two stress components at a defined stretch components, λ_θ and λ_z. Additionally, λ_θ can induce a change in λ_z, and this change is related to λ_θ by the following expression

$$\lambda_{z,\theta} = -\frac{c_1}{c_2 - \lambda_\theta} \tag{9}$$

The longitudinal stress shares the same form of Eq. (8) but with different constants c_3, c_4 and in terms of combined longitudinal stretch, $\lambda_z - \lambda_{z,\theta}$, namely

$$s_z = \frac{c_3}{\left(c_4 - \lambda_z - \lambda_{z,\theta}\right)^2} \tag{10}$$

Based on a series of experimental $s_\theta - \lambda_\theta$, $s_z - \lambda_z$ data, one can obtain model constants c_1 to c_4, then predict two stresses at a pair of λ_θ and λ_z by using the model above in a sequence of Eq. (7) to (10) and the expression $s_\theta = s_z f\left(\lambda_\theta\right)$. In the model, the hyperbola with power 2 exhibits a more compliant behaviour at low strains and a stiffer feature at high strains in venous walls.

4.2 Strain energy function methods

Strain energy function is a mathematical representation of strain energy stored in a deformed elastic body under the action of external forces in unit volume in terms of strains or their invariants. Usually, vascular soft tissues are viscoelastic and their stress-strain curve exhibits a hysteresis loop under a cyclic loading. To make the curve repeatable, a specimen of vascular soft tissue must experience a cyclic loading for a number of times before conducting uniaxial/biaxial tensile tests. This process is called preconditioning. The stress-strain curve of a preconditioned specimen is different from that of the un-preconditioned specimen, but is simpler in some degree than the latter. Thus this curve is pseudo elastic and the strain energy function for this curve is pseudo strain energy function [121]. Unless specially stated, the strain energy functions in following sections are pseudo elastic.

Six individual stain energy functions have been proposed and applied in biomechanical property modelling of venous walls, for example, two families of collagen fibres without orientation dispersion in [97], two families of fibres with different property constants in [122], two families of fibres with orientation dispersion [123] and four-family fibre without orientation dispersion [98], two families of fibres with anisotropic elastin and fibre recruitment [124], and its update version with fibre orientation [125]. The first four strain energy functions are deterministic, the last two are stochastic.

4.2.1 Two families of fibres without orientation dispersion

In [97], a strain energy function was proposed based on transversely isotropic, homogenous matrix material and two families of collagen fibres arranged axis-symmetrically about the arterial longitudinal axis. Two families of fibres share the same biomechanical property constants. The mathematical expression of the function is written as [97]

$$\psi = c\left(I_1 - 3\right) + \frac{k_1}{2k_2}\sum_{i=4,6}\left[e^{k_2\left(I_i-1\right)^2} - 1\right] \tag{11}$$

where the first invariant $I_1 = \lambda_r^2 + \lambda_\theta^2 + \lambda_z^2$, λ_r is the radial stretch, it yields the incompressible condition with the other stretch components, λ_θ and λ_z, namely $\lambda_r\lambda_\theta\lambda_z = 1$, the second invariants $I_4 = \lambda_\theta^2\cos^2\beta + \lambda_z^2\sin^2\beta$, $I_6 = \lambda_\theta^2\cos^2\left(-\beta\right) + \lambda_z^2\sin^2\left(-\beta\right)$, the angles, β and $-\beta$, are the mean fibre angle measured from the circumferential direction for two families of fibres.

The model expressed with Eq. (11) was used to determine matrix stiffness constant c, collagen fibre initial stiffness k_1, stiffness increasing rate k_2 and mean fibre orientation angle β from the Cauchy stress-stretch curves obtained in tubular biaxial inflation tests in [99, 100, 126]. Since the fibre orientation dispersion is not taken into account, the error in the stress between measurement and model prediction needs to be improved.

4.2.2 Two families of fibres with different property constants

Longitudinal and circumferential specimens cut from infrarenal vena cava of 15 lambs were measured by simple tensile test [122]. The Cauchy stress-stretch curves were fitted with three types of strain energy function without considering the collagen fibre orientation dispersion. The first strain energy function is Eq. (11). The second strain energy function is taken from [127], which is for rabbit left ventricular passive myocardium with one family of fibres, and then it is updated by adding another family of fibre. The updated strain energy function is read as follows [122]

$$\psi = c_1\left(e^Q + e^P - 1\right) \tag{12}$$

with

$$Q = c_2\left(I_1 - 3\right)^2 + c_3\left(I_1 - 3\right)\left(I_4 - 1\right) + c_4\left(I_4 - 1\right)^2 \tag{12a}$$

and

$$P = c_5\left(I_1 - 3\right)^2 + c_6\left(I_1 - 3\right)\left(I_6 - 1\right) + c_7\left(I_6 - 1\right)^2 \tag{12b}$$

where $c_2 > 0$, $c_4 > 0$, $c_5 > 0$, $c_7 > 0$, c_3 and c_6 are dimensionless, but c_1 is in stress unit. Note that expression P was added by the authors of [122]. The third type of stain energy function that was put forward in [122] is written as the following

$$\psi = c_1\left(I_1 - 3\right) + c_2\left(\sqrt{I_4} - 1\right)^2 + c_3\left(\sqrt{I_6} - 1\right)^2 \tag{13}$$

where c_1, c_2 and c_3 are positive property constant with stress unit.

It was shown that three models could fit the experimental data well [122], but the performance of the model in Eq. (12) was the best one; the rest models performed just satisfactorily with nearly equally large errors.

4.2.3 Two families of fibres with orientation dispersion

In reality, collagen fibre orientation does not direct a unique direction exactly; instead, the orientation is subject to dispersion. To consider this effect, the constitutive model, Eq. (11), was extended with fibre orientation dispersion [123], and the updated version of the strain energy function is written as,

$$\psi = c\left(I_1 - 3\right) + \frac{k_1}{2k_2}\sum_{i=4,6}\left[e^{k_2\left[\kappa\left(I_1-3\right)+\left(1-3\kappa\right)\left(I_i-1\right)\right]^2} - 1\right] \tag{14}$$

where κ is the fibre orientation dispersion coefficient, κ =0-0.33, it can be obtained by microscope observation or inversely determined along with the other constants c, k_1, k_2 and β based on known stress-stretch curves in the circumferential and longitudinal directions.

A series of specimens of murine inferior vena cava under normal and post-phlebitic conditions were tested on a custom-built biaxial mechanical testing device [128]. The strain energy function, Eq. (14), was applied to fit the experimental stress-stretch curves, and five model constants were extracted/optimized and compared between the healthy and diseased groups and the results were encouraging.

4.2.4 Four families of fibres model without orientation dispersion

Based on the constitutive law in Eq. (11), the two families of collagen fibres were taken by four families of fibres (two diagonally, one circumferentially, and one longitudinally) to reduce the errors in fitting pressure-radius and axial force-radius curves of porcine jugular veins [98]. The first term in Eq.(11) remains unchanged. Then the strain energy function takes the following form

$$\psi = c\left(I_1 - 3\right) + \frac{k_1}{2k_2}\sum_{i=4,6}\left[e^{k_2\left(I_i-1\right)^2} - 1\right] + \frac{k_{1i}}{2k_{2i}}\sum_{i=\theta,z}\left[e^{k_{2i}\left(\lambda_i^2-1\right)^2} - 1\right] \tag{15}$$

where k_{1i} and k_{2i} are the property constants for the circumferential and longitudinal fibres, respectively, i.e. $i=\theta,z$. It was stated that the arrangement of four families of collagen fibres was consistent with vein angioarchitecture observed histologically [98].

Similarly, the noe-Hookean term in Eq. (15) could be replaced with a quadratic function of two strain components to handle the response of elastin and are written as follows [98]

$$\psi = b_1E_\theta^2 + b_2E_z^2 + b_3E_\theta E_z + \frac{k_1}{2k_2}\sum_{i=4,6}\left[e^{k_2\left(I_i-1\right)^2} - 1\right] + \frac{k_{1i}}{2k_{2i}}\sum_{i=\theta,z}\left[e^{k_{2i}\left(\lambda_i^2-1\right)^2} - 1\right] \tag{16}$$

where E_θ and E_z are the circumferential and longitudinal strain components, and related to the circumferential and longitudinal stretch components, λ_θ and λ_z, with $E_\theta = 0.5\left(\lambda_\theta^2 - 1\right)$ and $E_z = 0.5\left(\lambda_z^2 - 1\right)$; b_1 to b_3 are model constants inversely determined based on experimental data.

It was demonstrated that the models in Eqs. (15) and (16) performed equally better than the Fung's model proposed in [121].

4.2.5 Two families of fibres with anisotropic elastin and fibre recruitment

For rat carotid artery in passive state, a constitutive model was developed [129]. In the model, it was considered that the arterial wall was composed of isotropic and homogenous matrix of elastin and two families of collagen fibres with mean orientation angles, β and $-\beta$, with respect to the circumferential direction. The fibres engage in tension based on a recruitment process. The strain energy function is written as [129]

$$\psi = f_{elast} c\left(I_1 - 3\right)^{3/2} + f_{coll} \sum_{i=4,6} \left[\frac{1}{2} \int_{-\infty}^{+\infty} \psi_{fibre}\left(x\right) \rho_{fibre}\left(\varepsilon_i - x\right) dx \right] \tag{17}$$

where f_{elast} and f_{coll} are the area fractions of elastin and collagen fibre in the tissue, respectively, f_{elast} =0.306 and f_{coll} =0.203 for rat carotid arterial wall, c is property constant of the elastin, ε_i is the strain of fibres in two families, $\varepsilon_i = \sqrt{I_i} - 1$, i =4, 6, ψ_{fibre} is the strain energy function of an individual collagen fibre and takes the following form [129]

$$\psi_{fibre}\left(\varepsilon_i\right) = \begin{cases} 0 & \text{for } \varepsilon_i \le \varepsilon_0 \\ c_{coll}\left[\varepsilon_i - \log\left(\varepsilon_i + 1\right)\right] & \text{for } \varepsilon_i > \varepsilon_0 \end{cases} \tag{18}$$

where c_{coll} is the Young's modulus of the collagen fibre, c_{coll} =200MPa, ε_0 is the fibre straightening strain at which a collagen fibre gets into tension, ε_0 =0 (WI=1) [129]. ρ_{fibre} is a log-logistic probability distribution function of fibre strain to regulate the fibre recruitment process and expressed by

$$\rho_{fibre}\left(\varepsilon_i\right) = \begin{cases} 0 & \text{for } \varepsilon_i \le \varepsilon_0 \\ \left(\frac{k}{b}\right) \frac{\left(\varepsilon_i - \varepsilon_0 / b\right)^{k-1}}{\left[1 + \left(\varepsilon_i - \varepsilon_0 / b\right)^k\right]^2} & \text{for } \varepsilon_i > \varepsilon_0 \end{cases} \tag{19}$$

where b (>0) is a scaling parameter and k (>0) defines the shape of ρ_{fibre}. The four constants c, β, k and b are determined inversely with experimental data in tubular biaxial vessel segment inflation tests.

It was observed that the longitudinal stress-strain curve of elastin was stiffer than the circumferential curve, showing an anisotropic property in the longitudinal direction [124]. To involve

this effect, the first term in Eq. (17) is replaced with additional term and the last term remains unchanged, then the following strain energy function is resulted

$$\psi = f_{elast} c\left(I_1 - 3\right)^{3/2} + f_{elast} c_1 \left(\lambda_z^2 + \frac{2}{\lambda_z} - 3 \right) + f_{coll} \sum_{i=4,6} \left[\frac{1}{2} \int_{-\infty}^{+\infty} \psi_{fibre}\left(x\right) \rho_{fibre}\left(\varepsilon_i - x\right) dx \right] \tag{20}$$

where five constants c, c_1, β, k and b are decided inversely with experimental data in tubular biaxial inflation tests of facial vein segments of rabbits and a better result has been achieved [124].

4.2.6 Two families of fibres with anisotropic elastin, fibre recruitment and orientation dispersion

In Eq. (20), the collagen fibre orientation dispersion is excluded. In reality, collagen fibres do not orientate one direction exactly; instead they orientate various directions by deviating from the mean orientation. To take this effect into account, the constitutive law presented by Eq. (20) was updated with fibre orientation dispersion, while the two terms for the elastin response remained unchanged [125]. Here just the modified stain energy function of collagen fibres is illustrated [125].

For two given Green strain components in a cylinder wall, such as E_θ and E_z, the strain along a fibre, which is subject to a fibre angle β measured from the circumferential direction, is written as

$$E_f = E_\theta \cos^2 \beta + E_z \sin^2 \beta \tag{21}$$

The true strain along the fibre with respect to the fibre straightening strain ε_0 is calculated by

$$\varepsilon_f = \frac{E_f - \varepsilon_0}{E_f + 2\varepsilon_0} \tag{22}$$

where $\varepsilon_0 = 0.5\left(\lambda_0^2 - 1\right)$, λ_0 is the fibre straightening stretch, λ_0 =WI, is a stochastic variable in a soft tissue, can be measured by microscope and yields the same probability density distribution as Eq. (19), then the fibre recruitment process is specified by

$$\rho_{fibre}\left(\varepsilon_f\right) = \begin{cases} 0 & \text{for } \varepsilon_f \le \varepsilon_0 \\ \left(\frac{k}{b}\right) \dfrac{\left(\varepsilon_f - \varepsilon_0/b\right)^{k-1}}{\left[1 + \left(\varepsilon_f - \varepsilon_0/b\right)^k\right]^2} & \text{for } \varepsilon_f > \varepsilon_0 \end{cases} \tag{23}$$

The fibre is a linear material with a modulus c_{coll} and its strain energy function is in the following form

$$\psi_{fibre}\left(\varepsilon_f\right) = \begin{cases} 0 & \text{for } \varepsilon_f \le \varepsilon_0 \\ \frac{1}{2} c_{coll} \varepsilon_f^2 & \text{for } \varepsilon_f > \varepsilon_0 \end{cases} \tag{24}$$

Then the strain energy function of the fibre with the fibre angle β is calculated by the flowing equation when the recruitment is considered

$$\psi_{fibre}^{\beta}\left(\varepsilon_f\right)=\int_0^{E_f}\rho_{fibre}\left(\varepsilon_0\right)\psi_{fibre}\left(\varepsilon_f\right)d\varepsilon_0 \tag{25}$$

Finally, the strain energy function of one family of fibres will be estimated by integrating Eq. (25) with respect to $\psi_{fibre}^{\beta}\left(\varepsilon_f\right)$ and fibre orientation distribution function $R(\beta)$ in the following expression

$$\psi_{fibre}^{\bar{\beta}}\left(\varepsilon_f,\bar{\beta}\right)=\int_0^{\pi}\int_0^{E_f}\rho_{fibre}\left(\varepsilon_0\right)\psi_{fibre}\left(\varepsilon_f\right)R(\beta)d\varepsilon_0 d\beta=\tfrac{1}{2}c_{coff}\int_0^{\pi}\int_0^{E_f}\rho_{fibre}\left(\varepsilon_0\right)\varepsilon_f^2R(\beta)d\varepsilon_0 d\beta \tag{26}$$

where $\bar{\beta}$ is the mean fibre angle, $R(\beta)$ is the planar π-periodic von-Mises distribution for fibre orientation profile, i.e.

$$R\left(\beta,\bar{\beta},a\right)=\frac{1}{\pi I_0\left(a\right)}e^{a\cos\left[2\left(\beta-\bar{\beta}\right)\right]},\ I_0\left(a\right)=\frac{1}{2\pi}\int_0^{2\pi}e^{a\cos\beta}d\beta,\ \beta\in[0,\pi] \tag{27}$$

where $\bar{\beta}$ and a are fibre structure parameters and can be determined by fitting histologically experimental β profiles.

The strain energy function of the other one family of fibres with a $-\bar{\beta}$ mean fibre angle and the same parameter a is identical to Eq. (26). As such the updated stain energy function is written

$$\psi=f_{elast}c\left(I_1-3\right)^{3/2}+f_{elast}c_1\left(\lambda_z^2+\frac{2}{\lambda_z}-3\right)+f_{coll}c_{coff}\int_0^{\pi}\int_0^{E_f}\rho_{fibre}\left(\varepsilon_0\right)\varepsilon_f^2R(\beta)d\varepsilon_0 d\beta \tag{28}$$

This strain energy function has been used to fit the pressure-radius, pressure-axial force experimental data of rabbit facial vein segment and a good result was achieved [125].

Note that the strain energy functions in Eqs.(20) and (28) are quite time-consuming due to the integrals involved in comparison with those in Eqs.(11) to (16). Thus two functions Eqs.(20) and (28) might not be applicable in FEA simulations.

4.3 Applications of constitutive law

4.3.1 Image-based *in vivo* property constants determination

Ultrasound images of femoral vein of healthy 40year-old volunteer were captured in real time, and registered by using a time sequence of 10s. The intraluminal pressure of the vein was recorded as well. The circumferential and longitudinal Cauchy stresses were estimated by using thin-walled model without residual strain [130].

The constitutive law Eq. (11) was simplified by assuming that there was one family of fibres only in the femoral vein wall, then a method was designed to estimate remaining four model parameters based on clinically observed instant pressure and inner diameter of femoral vein and a constant longitudinal stretch 1.08. The predicted inner diameter of formal vein is compared with the diameters from the images in Fig. 12. Since the viscoelastic property of the vein wall was not taken into account, the model prediction was a single-line curve only.

4.3.2 FEA of junction of vein graft with artery

A computational method for simulating CABG surgery was proposed, and effects of two clinically parameters, such as incision length and insertion angle on artery and graft responses, were analysed at a fixed graft diameter, based on actual 3D vessel dimensions of a human coronary artery and a saphenous vein [131]. The end-to-side anastomosis structure, residual stresses, anisotropic and nonlinear feature of blood vessels were considered. The coronary artery was a three-layer thick-walled cylinder.

A series of FEA simulations were performed to predict deformation and stress distribution in the end-to-side anastomosis at various stages of CABG surgery. It was shown that the arterial incision had a significant effect on the size of the arterial opening, depending on the residual stress only. The incision length influenced critically the graft shape and the stress level in the graft wall. Stress level in the heel region was higher than in the toe region, see Fig. 13 and 14. A stress concentration could be found at the incision ends.

The proposed computational methodology may be useful in designing a coronary anastomotic device to reduce surgical trauma. It may improve the quantitative knowledge of vessel diseases and serve as a tool for virtual planning of vascular surgery.

5 Discussions

5.1 Difference in stress-stretch curves

The biomechanical property of saphenous vein wall can be characterized *in vitro* by uniaxial and tubular biaxial tensile tests as shown in the previous sections. What is the difference in Cauchy stress-stretch curves in both tests for the human saphenous vein? In Fig. 15, a comparison of Cauchy-stretch curves is made for the human saphenous vein measured by two tensile tests. The tensile data of sample saphenous vein 2 (SV2) are taken from [64], while the first tubular biaxial inflation test data were measured in [99] at 4Hz loading rate on the human saphenous vein segments.

In comparison with the uniaxial tensile test results, the stress-stretch curves measured by the tubular biaxial inflation tests show more wide stretch range at a very low stress level, see Fig. 15. Which data group is mostly suitable for saphenous vein CABG under arterial physiological conditions? Obviously, this problem needs further research in the future.

5.2 Biomechanical property identification *in vivo*

It may be very significant for the diagnosis of disease in saphenous vein CABGs by characterizing the passive biomechanical property *in vivo*. Further, this characterization can involve the viscoelasticity of saphenous veins. Currently, this issue is little tackled in literature [101, 130]. More advanced devices and modelling methods are on demand presently.

5.3 Tissue damage effects

It was observed that the saphenous vein wall could be damaged when transmural pressure was in a range of 50-60mmHg [95]. Under coronary artery physiological conditions, the intraluminal pressure is higher than this pressure level, as such the tissue of human saphenous vein CABGs may be subject to damage or sub-failure. For the rat ligament, damage or sub-failure threshold in fibre stretch was 1.0514 [132]. What is the damage or sub-failure threshold for the human saphenous vein CABGs ? How to model the damage or sub-failure effect in the human saphenous vein CABGs by using constitutive laws ?

5.4 Residual strain/stress

In section 3.2.4, it is shown that the residual strain/stress does exist in the human saphenous vein. Currently, the mean opening angle is as high as 120^{o} for 15 patients [94] in comparison with an angle as low as 45^{o} of four patients [118]. Such a huge difference needs to be clarified with significant further observations in the future.

5.5 CABG Remodelling

After surgery, CABGs are subject to thickening and remodelling processes in coronary artery environment. These two processes are induced and regulated by blood shear stress applied on the graft wall and the stress in the wall under an increased intraluminal pressure load [133, 134]. The vein graft remodelling initiated by blood shear stress has been studied extensively, such as those in [135, 136].

Blood pressure in the left femoral vein of the rabbit was chronically elevated by the constriction in the left external iliac vein to clarify the changes in biomechanical properties caused by such a hypertension [137]. Wall thickness and active passive biomechanical properties of the vein were measured *in vitro* at 1, 2 and 4weeks after surgery. Wall thickness was increased even at 1week to restore circumferential wall stress to a control level. Vascular tone and contractility were intensified by the hypertension; however, wall incremental Young's modulus and compliance remained at a normal level. These results suggested that veins could remodel themselves against a raised blood pressure like arteries.

Interestingly, arteriovenous fistulas were generated by implanting e-PTFE grafts between carotid artery and jugular vein in healthy pigs under over-loaded flow and pressure conditions [138]. The wall thickening was exhibited in grafted vessels in 2weeks; the intramural stresses was restored to homeostatic levels, and the internal diameter enlargement got less, the intimal shear stress became normal gradually after 4weeks. The residual strains and opening angle increased at 12weeks. There was a correlation between intimal hyperplasia and opening angle increase. Elastin contents reduced but collagen contents increased within the first 4weeks. In vessel segment inflation tests, the vein walls showed a stiffer behaviour in comparison with the baseline levels. The experimental pressure-radius, axial force-radius data points of the post-fistula measured at 2, 4 and 12weeeks were fitted

with Eq. (16), and the extracted material constants were correlated to elastin and collagen contents observed [139]. This research methodology has provided a good idea for CABG remodelling problem.

At the moment, the wall stress factor is not involved in experiments and mathematical models in human venous graft remodelling. The saphenous vein CABG remodelling needs to be tackled experimentally and mathematically by involving shear stress on venous wall and stresses in the wall.

5.6 Regional Deformation and Material Properties

The biomechanical properties of human vein were not homogenous circumferentially and longitudinally, showing variable material properties and deformation from one region to another [140]. This heterogeneity has not been considered in saphenous vein CABG modelling and experiments so far. If this issue can be addressed in the near future, it will be beneficial to CABG design and surgery.

5.7 Applications of FEA in CABGs

FEA is an important method in biomechanical engineering, especially in biomechanics and its clinical application for soft tissue. In Section 4.3.2, it is seen that the cases of FEA for prediction of deformation and stress in CABGs are very lack. This may be caused from a little known about the constitutive law of layered human saphenous vein walls or complicated interaction between the coronary artery and a vein graft. Furthermore, the fluid-structure interaction in saphenous vein CABGs is little tackled at the moment as well.

6 Conclusions

Biomechanical properties of the human saphenous vein, which has been applied in blocked coronary artery to serve as a bypass graft and survive the diseased heart, were reviewed comprehensively in terms of active and passive mechanical behaviours. Particularly, the passive biomechanical properties have been extensively discussed by summarizing and interpreting existing *in vitro* uniaxial, bulge, planar and tubular biaxial tensile testing methods, *in vivo* test methods, property variables, various test results, constitutive laws and their mathematical modelling approaches, viscoelasticity, and residual strain/stress. It is shown that very limited attention has been paid to the biomechanical properties of the human saphenous vein and their modelling approaches need to be updated by considering the fibre orientation dispersion and sub-failure/damage effects in the tissue. The *in vivo* study on the biomechanical properties of the human saphenous vein is very rare. In the future, important research issues, such as the feasibility of constitutive laws under coronary artery physiological conditions based on uniaxial, tubular biaxial inflation test results of the human saphenous vein, biomechanical property identification *in vivo*, tissue damage effects, residual strain/stress identification, coronary artery bypass graft remodelling, regional deformation and material properties of coronary artery bypass graft, finite element analysis application in coronary artery bypass grafts have to be addressed.

Declaration of interest

There are no conflicts of interest.

Reference

[1] Diodato Ml and Chedrawy E G, Coronary Artery Bypass Graft Surgery: The Past, Present, and Future of Myocardial Revascularisation, doi: http://dx.doi.org/10.1155/2014/726158.

[2] Miller D W and Dodge H T, Benefits of coronary artery bypass surgery, Archives of Internal Medicine, 1977, 137: 1439-1446.

[3] http://www.nhs.uk/conditions/Coronary-artery-bypass/Pages/Introduction.aspx

[4] http://www.surgery.usc.edu/vascular/varicoseveinsandvenousdisease.html

[5] https://atlasofscience.org/a-novel-treatment-for-saphenous-venous-graft-thrombosis/

[6] Hassantash S A, Bikdeli B, Kalantarian S, Sadeghian M and Afshar H, Pathophysiology of aortocoronary saphenous vein bypass graft disease, Asian Cardiovascular & Thoracic Annals, 2008, 16(4): 331-336.

[7] Vlodaver Z and Edwards J E, Pathologic changes in aortic-coronary arterial saphenous vein grafts, Circulation, 1971, 44: 719-728.

[8] Walts A E, Fishbein M C, Sustaita H and Matloff J M, Ruptured atheromatous plaques in saphenous vein coronary artery bypass grafts: a mechanism of acute, thrombotic, late graft occlusion, Circulation, 1982, 65: 197-201.

[9] Cooper G J, Underwood M J and Deverall P B, Arterial and venous conduits for coronary artery bypass, European Journal of Cardio-Thoracic Surgery, 1996, 10: 129-140.

[10] Ramirez F D, Hibbert B, Simard T, Pourdjabbar A, Wilson K R, Hibbert R, Kazmi M, Hawken S, Ruel M, Labinaz M and O'Brien E R, Natural history and management of aortocoronary saphenous vein graft aneurysms, Circulation, 2012, 126:2248-2256.

[11] de Vries M R, Simons K H, Jukema J W, Braun J and Quax H A, Vein graft failure: from pathophysiology to clinical outcomes, Nature Reviews, 2016, 13:451-470.

[12] Zachrisson H, Lindenberger M, Hallman D, Ekman M, Neider D and Lanne T, Diameter and compliance of the greater saphenous vein-effect of age and nitro-glycerine, Clinical Physiology and Functional Imaging, 2011, 31: 300-306.

[13] Pourdeyhimi B and Text C, A review of structural and material properties of vascular grafts, Journal of Biomaterials Application, 1987; 2: 163-204.

[14] Brossollet L J, Mechanical issues in vascular grafting: a review, International Journal of Artificial Organs, 1992, 115(10): 579-584

[15] Salacinski H J, Goldner S, Giudiceandrea A, Hamilton G and Seifalian A M, The mechanical behaviour of vascular grafts: a review, Journal of Biomaterials Applications, 2001, 15: 241-278.

[16] Kannan R Y, Salacinski H J, Butler P E, Hamilton G and Seifalian A M, Current status of prosthetic bypass grafts: a review, Journal of Biomedical Materials Research Part B: Applied Biomaterials, 2005, 74B(1): 570–581.

[17] Snowhill P B and Silver F H, A mechanical model of porcine vascular tissues-Part I: determination of macromolecular component arrangement and volume fractions, Cardiovascular: An International Journal, 2005, 4: 281-294.

[18] Spary T L and Roberts W C, Changes in saphenous veins used as aortocoronary bypass grafts, Fundamentals of Clinical Cardiology, 1977, 94: 500-516.

[19] Thine G, Miazzi P, Valsecchi M, Valente M, Bortolotti U, Casarotto D and Gallucci V, Histological survey of the saphenous vein before its use as autologous aortocoronary bypass graft, Thorax, 1980, 35: 519-522.

[20] Milroy C , Scott D J A, Beard J D, Horrocks M and Bradfield W B, Histological appearance of the saphenous vein, Journal of Pathology, 1989, 159: 311-316.

[21] Naim M M and Elsharawy M, Histological assessment of the long saphenous vein in normal and varicose veins, The Egyptian Journal of Histology, 2005, 28: 281-290.

[22] Burton A C, Relation of structure to function of the tissues of the wall of blood vessels, Physiological Reviews, 1954, 34: 619-642.

[23] Vesely J, Hadraba D, Chlup H, Horny L, Adamek T and Zitny, Constitutive modelling and histological of vena saphena, Applied Mechanics and Materials, 2014, 486: 249-254.

[24] Wolinsky H and Glagov S, Structural basis for the static mechanical properties of the aortic media, Circulation Research, 1964, 14: 400-413.

[25] Sokolis D P, Passive mechanical properties and constitutive modeling of blood vessels in relation to microstructure, Biomechanics Modeling and Mechanobiology, 2008, 46(12): 1187-99.

[26] Vesely J, Horny L, Chlup H and Zitny R, Collagen orientation and waviness within the vein wall, Proceedings of the 11th International Conference on Computational Plasticity: Fundamentals and Applications, Onate E, Owen D R J, Peric D and Suarez B (eds), Barcelona, Spain, 7-9 September 2011: 720-728.

[27] Rezakhaniha R, Agianniotis A, Schrauwen, Griffa A, Sage D, Bouten C V C, van de Vosse F N , Unser M and Stergiopulos N, Experimental investigation of collagen waviness and orientation in the arterial adventitia using confocal laser scanning microscopy, Biomechanics Modeling and Mechanobiology, 2012, 11: 461-473.

[28] Svejcar J, Prerovsky I, Linhart J and Kruml J, Content of collagen, elastin and water in walls of the internal saphenous vein in man, Circulation Research, 1962, 11: 296-300.

[29] Kransinski Z, Bikupski P, Dzieciuchowicz L, KaczmarekE, Krasinska B, Staniszewski R, Oawlaczyk K, Stanisic M, Majewski P and Majewski W, The influence of elastic components of the venous wall on the biomechanical properties of different veins used for arterial reconstruction, European Journal of Endovascular Surgery, 2010, 40: 224-229.

[30] Psaila J V and Mehuish J, Viscoelastic properties and collagen content of the long saphenous vein in normal and varicose veins, British Journal of Surgery, 1989, 76, 37-40.

[31] Haviarová Z, Weismann P, Štvrtinová V, Beňuška J, The determination of the collagen and elastin amount in the human varicose vein by the computer morphometric method, General Physiology and Biophysics, 1999, 18(Supplement 1): 30-33.

[32] MacWilliam J A, On the properties of the arterial and venous walls, Proceedings of the Royal Society of London, 1902, 70: 109-153.

[33] Alexander R S, Contractile mechanics of venous smooth muscle, American Journal of Physiology, 1967, 212(4): 852-858.

[34] Alexander R S, Role of calcium in the plasticity of venous smooth muscle, American Journal of Physiology, 1967, 213(1): 287-294.

[35] Venhoutte P and Leusen I, The reactivity of isolated venous preparations to electrical stimulations, Pflugers Archiv, 1969, 306: 341-353.

[36] Vanhoutte P M and Lorenz R R, Effect of temperature on reactivity of saphenous, mesenteric and femoral veins of the dog, American Journal of Physiology, 1970, 218(6): 1746-1750.

[37] Schoeffter P and Godfraind T, Spontaneous rhythmic contractions of human saphenous veins isolated from old subjects are sensitive to cyclooxygenase inhibitors, Experientia, 1989, 45: 459-461.

[38] Hill-Eubanks D C, Werner M E, Heppner T J and Nelson M T, Calcium signalling in smooth muscle, Cold Spring Harbor Perspectives in Biology, 2011, 3: 1-20.

[39] Amberg G C and Navedo M F, Calcium dynamics in vascular smooth muscle, Microcirculation, 2013, 20(4): 281-289.

[40] Crowley C M, Lee C H, Gin S A, Keep A M, Cook R C and Van Breemen C, The mechanism of excitation-contraction coupling in phenylephrine-stimulated human saphenous vein, American Journal of Physiology Heart Circulation Physiology, 2002, 283: H1271-H1281.

[41] Gestrelius S and Borgstrom P, A dynamic model of smooth muscle contraction, Biophysical Journal, 1986, 50: 157-169.

[42] Liu T, A constitutive model for cytoskeletal contractility of smooth muscle, Proceedings of the Royal Society, Series A, 2013, 470: 20130771.

[43] Kim J and Wagenseil J E, Bio-chemo-mechanical models of vascular mechanics, Annals of Biomedical Engineering, 2015, 43(7): 1477-1487.

[44] Seidel C L, Lewis R M, Bowers R, Bukoski R D, Kim H S, Allen J C and Hartley C, Adaptation of Canine Saphenous Veins to Grafting, Circulation Research, 1984, 55(1): 102-109.

[45] Park T C, Harker C T, Edwards J M, Moneta G L, Taylor L M and Porter J M, Human saphenous vein grafts explanted from the arterial circulation demonstrate altered smooth-muscle and endothelial responses, Journal of Vascular Surgery, 1993, 1(1): 61-69.

[46] Sanchez A M, Wooldridge T A, Boerboom L E, Olinger G N, Almassi G H and Rusch N, Comparison of saphenous vein graft relaxation between Plasma-Lyte solution and norm.al saline solution, The Journal of Thoracic and Cardiovascular Surgery, 1994, 107(6): 1445-1453.

[47] Beattiet D K, Gosling M, Davies A H and Powelll J T, The effects of potassium channel openers on saphenous vein exposed to arterial flow, European Journal of Vascular & Endovascular Surgery, 1998, 15: 244-249.

[48] McGregor E, Gosling M, Beattie D K, Ribbons D M P, Davies A H and Powell J T, Circumferential stretching of saphenous vein smooth muscle enhances vasoconstrictor responses by Rho kinase-dependent pathways, Cardiovascular Research, 2002, 53: 219–226.

[49] Borna C, Wang L, Gudbjartsson T, Karlsson L Jern S, Malmsjo M and Erlinge D, Contractions in human coronary bypass vessels stimulated by extracellular nucleotides, Annals Thoracic Surgery, 2003;76:50-57.

[50] Okon E B, Millar M J, Crowley C M, Bashir J G, Cook R C, Hsiang Y N, McManus B, and van Breemen C, Effect of moderate pressure distention on the human saphenous vein vasomotor function, Annals Thoracic Surgery, 2004, 77: 108–15.

[51] Khalil A, El-Bayar M and Molokhia F, Dispensability of isolated segments of femoral and saphenous veins, Angiology, 1968, 19(7): 419-425.

[52] Baird R N, Kindson I G, L'Italien G J and Abbott W M, Dynamic compliance of arterial grafts, American Journal of Physiology, 1977, 233(5): H568-H572.

[53] Hildebrandt J H, Fukaya H and Martin C J, Stress-strain relations of tissue sheets undergoing uniform two-dimensional stretch, Journal of Applied Physiology, 1969, 27(5): 758-762.

[54] Baird R N and Abbott W M, Elasticity and compliance of canine femoral and jugular vein segments, American Journal of Physiology, 1977, 233(1): H15-H21.

[55] Wesly R L R, Vaishnav R N, Fuchs J A, Patel D J and Greenfield C, Static linear and nonlinear elastic properties of normal and arterialized venous tissue in dog and man, Circulation Research, 1975, 37: 509-520.

[56] Cox R H, Three-dimensional mechanics of arterial segments in vitro: methods, Journal of Applied Physiology, 1974, 36(3): 381-384.

[57] Fronek K, Schmid-Schoenbein G and Fung Y C, A noncontact method for three-dimensional analysis of vascular elasticity in vivo and vitro, Journal of Applied Physiology, 1976, 40(4): 634-637.

[58] Weizsacker H W, Passive elastic properties of the rat abdominal vena cava, Pflugers Archiv-European Journal of Physiology, 1988, 412: 147-154.

[59] Tonge T K, Atlan L S, Voo L M and Nguyen T D, Full-field bulge test for planar anisotropic tissues: Part I-experimental methods applied to human skin tissue, Acta Biomaterialia, 2013, 9: 5913-5923.

[60] Tonge T K, Atlan L S, Voo L M and Nguyen T D, Full-field bulge test for planar anisotropic tissues: Part II-a thin shell method for determining material parameters and comparison of two distribution fiber modelling approaches, Acta Biomaterialia, 2013, 9: 5926-5942.

[61] Attinger F M L, Two-dimensional in-vitro studies of femoral arterial walls of the dog, Circulation Research, 1968, 22:829-840.

[62] Silver F H, Snowhill P B and Foran D J, Mechanical behaviour of vessel wall: a comparative study of aorta, vena cava, and carotid artery, Annals of Biomedical Engineering, 2003, 31:793-803.

[63] Snowhill P B and Silver F H, A mechanical model of porcine vascular tissues-Part II: stress-strain and mechanical properties of juvenile porcine blood vessels, Cardiovascular: An International Journal, 2005, 5: 157-169.

[64] Hamedani B A, Navidbakhsh M and Tafti H A, Comparison between mechanical properties of human saphenous vein and umbilical vein, BioMedical Engineering Online, 2012, 11: 59-74.

[65] Lanir Y and Fung Y C, Two-dimensional mechanical properties of rabbit skin-I. Experimental system, Journal of Biomechanics, 1974, 7: 29-34.

[66] Lanir Y and Fung Y C, Two-dimensional mechanical properties of rabbit skin-II. Experimental results, Journal of Biomechanics, 1974, 7: 171-182.

[67] Sacks M S, Biaxial mechanical evaluation of planar biological materials, Journal of Elasticity, 2000, 61: 199-246.

[68] Fehervary H, Smoljkic M, Sloten J V and Famaey N, Planar biaxial testing of soft biological tissue using rakes: Acritical analysis of protocol and fitting process, Journal of the Mechanical Behavior of Biomedical Materials, 2016, 61: 135-151.

[69] Keyes J T, Lockwood D R, Utzinger U, Montilla L G, Witte R S and Vande Geest J P, Comparisons of planar and tubular biaxial tensile testing protocols of the same porcine coronary arteries, Annals of Biomedical Engineering, 2013, 41: 1579-1591.

[70] Clark J H, The elasticity of veins, American Journal of Physiology, 1933, 105:418-427.

[71] Brown B P and Heistad D D, Capacitance of the rabbit portal vein and inferior vena cava, Journal of Physiology, 1986, 381: 417-425.

[72] Beard J D and Fairgrieve J, Compliance changes in in-situ femoropopliteal bypass vein grafts, British Journal of Surgery, 1986, 73: 196-199.

[73] Abbott W M, Megerman J, Hasson J E, L'Italien G and Warnock D F, Effect of compliance mismatch on vascular graft patency, Journal of Vascular Surgery, 1987, 5(2): 376-382.

[74] Walden R, L'Italien G J, Megerman J and Abbott W M, Matched elastic properties and successful arterial grafts, Archives of Surgery, 1980, 115: 1165-1169.

[75] Kidson I G, The effect of wall mechanical properties on patency of arterial grafts, Annals of the Royal College of Surgeons of England, 1983, 65: 24-29.

[76] Tai N R, Salacinski H J, Edwards A, Giudiceandrea A, Hamilton G and Seifalian A M, Compliance properties of conduits used in vascular reconstruction, British Journal of Surgery, 2000, 87: 1516-1524.

[77] Young C N, Stillabower M E, DiSabatino A and Farquhar B, Venous smooth muscle tone and responsiveness in older adults, Journal of Applied Physiology, 2006, 101: 1362-1367.

[78] Young C N, Prasad R Y, Fullenkamp A M, Stillbower M E, Farquhar B and Edwards D G, Ultrasound assessment of popliteal vein compliance during a short deflation protocol, Journal of Applied Physiology, 2008, 104: 1374-1380.

[79] Zachrisson H, Lindenberger M, Hallman D, Ekman M, Neider D and Lanne T, Diameter and compliance of the greater saphenous vein-effect of age and nitroglycerine, Clinical Physiology and Functional Imaging, 2011, 31(4): 300-306.

[80] Bocking J K and Roach M R, The effects of hydrostatic pressure on the elastic properties of cat veins, Canadian Journal of Physiology and Pharmacology, 1974, 52:148-151.

[81] Bocking J K and Roach M R, The elastic properties of the human great saphenous vein in relation to primary varicose veins, Canadian Journal of Physiology and Pharmacology, 1974, 52:153-157.

[82] Dobrin P B, Littooy F N, Golan J, Blakeman B and Fareed J, Mechanical and histologic changes in canine vein grafts, Journal of Surgical Research, 1988, 44:259-265.

[83] Angelini G D, Passani S L, Breckenridge I M and Newby A C, Nature and pressure dependence of damage induced by distension of human saphenous vein coronary artery bypass grafts, Cardiovascular Research, 1987, 21:902-907.

[84] Hofstra L, Bergmans D C J J, Hoeks A P G, Tordoir J H M and Kitslaar P J E H M, Assessment of inhomogeneity in elastic properties of in situ and reversed saphenous vein grafts in humans, European Journal of Vascular Surgery, 1994, 8: 670-676.

[85] Stooker W, Gok M, Sipkema P, Niessen H W M, Baidoshvili A, Westerhof N, Jansen E K, Wildevuur C R H and Eijsman L, Pressure-diameter relationship in the human greater saphenous vein, Annals of Thoracic Surgery, 2003, 76: 1533-1538.

[86] Paranjothi K, Saravanan U, KrishnaKumar R and Balakrishnan K R, Mechanical Properties of Human Saphenous Vein, Mechanics of Biological Systems and Materials-Volume 2, New York: Springer 2011: 79-85.

[87] Forouzandeh F, Bozorgi M H, Meshkat B and Fatouraee N, Measurement of mechanical properties of human saphenous vein using an inflation experiment, Proceedings of 20th Iranian Conference on Biomedical Engineering (ICBME 2013), University of Tehran, Tehran, Iran, December 18-20, 2013.

[88] Voishnav R N, Young J T and Patel D J, Distribution of stresses and of strain-energy density through the wall thickness in a canine aortic segment, Circulation Research, 1973, 32: 577-583.

[89] Attinger E O, Wall properties of veins, IEEE Transactions on Bio-medical Engineering, 1969, 16: 253-261.

[90] Sakanish A, Hasegawa M and Dobashi T, Distensibility characteristics of caval veins and empirical exponential formulae, Biorheology, 1988, 25(1-2): 165-172.

[91] Donovan D L, Schmidt S P, Townshend S P, Njus G O and Sharp W V, Material and structural characterization of human saphenous vein, Journal of Vascular Surgery, 1990, 12: 531-537.

[92] Rossman J S, Elastomechanical properties of bovine veins, Journal of the Mechanical Behavior of Biomechanical Materials, 2010, 3: 210-215.

[93] Rassoli A, Fatouraee N and Shafigh M, Uniaxial and biaxial mechanical properties of the human saphenous vein, Biomedical Engineering: Applications, Basis and Communications, 2015, 27(5): 1-10.

[94] Zhao J B, Andersen J J, Yang J, Rasmussen B S, Liao D H and Gregersen H, Manual pressure distension of the human saphenous vein changes its biomechanical properties-implication for coronary artery bypass grafting, Journal of Biomechanics, 2007, 40: 2268-2276.

[95] Ozturk N, SuCu N, Comelekoglu U, Yilmaz B C and Aytacoglu B N, Pressure applied during surgery alters the biomechanical properties of human saphenous vein graft, Heart Vessels, 2013, 28: 237-2245.

[96] Lee Y U, Naito Y, Kurobe H, Breuer C K and Humphrey J D, Biaxial mechanical properties of the inferior vena cava in C57BL/6 and CB-17 SCID/bg mice. Journal of Biomechanics, 2013, 46(13): 2277-2282.

[97] Holzapfel G, Gasser T and Ogden R, A new constitutive framework for arterial wall mechanics and a comparative study of material models, Journal of Elasticity, 2000, 61: 1-48.

[98] Sokolis D P, Experimental investigation and constitutive modelling of the 3D histomechanical properties of vein tissue, Biomechanics Modeling and Mechanobiology, 2013, 12: 431-451.

[99] Vesely J, Horny L, Chlup H and Zitny R, Inflation tests of vena saphena maga for different loading rates, In: Proceedings of 13th Mediterranean Conference on Medical and Biological Engineering and Computing, IFMBE Proceedings, Roa Romero L. (eds) Vol. 41. Springer, Cham, 2014: 1041-1044.

[100] Vesely J, Horny L, Chlup H, Adamek T, Krajicek M and Zitny, Constitutive modelling of human saphenous veins at overloading pressures, Journal of the Mechanical Behavior of Biomedical Materials, 2015, 45: 101-108.

[101] Bauer R D, Busse R, Schabeer A, Summa Y and Wetterer E, Separate determination of the pulsatile elastic and viscous forces developed in the arterial wall in vivo, European Journal of Physiology, 1979, 380: 221-226.

[102] Zsoter T and Cronin R F P, Venous distensibility in patients with varicose veins, The Canadian Medical Association Journal, 1966, 94(25): 1293-1297.

[103] Hasegawa M, Rheological properties and wall structures of large veins, Biorheology 1983, 20: 531-45.

[104] Remington J W, Hysteresis loop behaver of the aorta and other extensible tissues, American Journal of Physiology, 1955, 180: 83-95.

[105] Goto M and Kimoto Y, Hysteresis and stress-relaxation of the blood vessels studied by a universal tensile testing instrument, The Japanese Journal of Physiology, 1966, 15: 169-184.

[106] Lee J M, Wilson G J, Anisotropic tensile viscoelastic properties of vascular graft materials tested at low strain rates, Biomaterials, 1986, 7(6): 423-31.

[107] Abramowitch S D and Woo S L Y, An improved method to analyze the stress relaxation of ligaments following a finite ramp time based on the quasi-linear viscoelastic theory, Journal of Biomechanical Engineering, 2004, 126: 92-97.

[108] Kohandel M, Sivaloganthan S and Tenti G, Estimation of the quasi-linear viscoelastic parameters using genetic algorithm, Mathematical and Computer Modelling, 2008, 47: 266-270.

[109] Aisa R, Arezu A M, Nasser F, Saeed S A and Mohammad S, A structural constitutive model for viscoelastic rheological behavior of human saphenous vein using experimental assays, International Journal of Medical, Health, Biomedical, Bioengineering and Pharmaceutical Engineering, 2016, 10(3): 170-173.

[110] Rachev A and Greenwald S E, Residual strains in conduit arteries, Journal of Biomechanics, 2003, 36: 661-670.

[111] Fung Y C and Liu S Q, Strain distribution in small blood vessels with zero-stress state taken into consideration, American Journal of Physiology, 1992, 262: H544-H552.

[112] Xie J P, Zhou J B and Fung Y C, Bending of blood vessel wall: Stress-strain laws of the intima-media and adventitial layers, Journal of Biomechanical Engineering, 1995, 117: 136-145.

[113] Chuong C J and Fung Y C, On residual stresses in arteries, Journal of Biomechanical Engineering, 1986, 108: 189-192.

[114] Labrosse M R, Gerson E R, Veinot J P and Beller C J, Mechanical characterization testing and a paradigm shift for circumferential residual stress, Journal of the Mechanical Behavior of Biomedical Materials, 2013, 17: 44-55.

[115] Xie J P, Liu S Q, Yang R F and Fung Y C, The zero-stress state of rat veins and vena cava, Journal of Biomechanical Engineering, 1991, 113: 36-41.

[116] Pang Q, Lu X, Gregersen H, von Oettingen G and Astrup J, Biomechanical properties of porcine cerebral bridging vein with reference to the zero-stress state, Journal of Vascular Research, 2001, 38: 83-90.

[117] Huang W and Yen R T, Zero-stress states of human pulmonary arteries and veins, Journal of Applied Physiology, 1998, 85(3): 867-873.

[118] Vesely J, Horny L, Chlup H, Adamek T and Zitny R, Opening angle of human saphenous vein, Proceedings of the 13th International Conference on Computational Plasticity: Fundamentals and Applications, Onate E, Owen D R J, Peric D and Chiumenti M (eds), Barcelona, Spain, 1-3 September 2015: 457-462.

[119] Han H C, Zhao L, Huang M, Hou L S, Huang L S and Kuang Z B, Postsurgical changes of the opening angle of canine autogenous vein graft, Journal of Biomechanical Engineering, 1998, 120: 211-216.

[120] Desch G W and Weizsacker H W, A model for passive elastic properties of rat vena cava, Journal of Biomechanics, 2007, 40: 3130-3145.

[121] Fung Y C, Fronek K and Patitucci P, Pseudoelasticityof arteries and the choice of its mathematical expression, American Journal of Physiology, 1979, 237(5): H620-H631.

[122] Alastrue V, Pena E, Martinez M A and Doblare M, Experimental study and constitutive modelling of the passive mechanical properties of the ovine infrarenal vena cava, Journal of Biomechanics, 2008, 41: 3038-3045.

[123] Gasser T, Ogden R and Holzapfel G, Hyperplastic modelling of arterial layers with distributed collagen fibre orientations, Journal of the Royal Society Interface, 2006, 3: 15-35.

[124] Rezakhaniha R and Stergiopulos N, A structure model of the venous wall considering elastin anisotropy, Journal of Biomechanical Engineering, 2008, 130: 031017-1-11.

[125] Agianniotis A, Rezakhaniha R and Stergiopulos N, A structure model considering angular dispersion and waviness of collagen fibres of rabbit facial veins, BioMedcial Engineering Online, 2011, 10: 1-18.

[126] Vesely J, Hadraba D, Chlup H, Horny L, Adamek T and Zitny, Constitutive modelling and histological of vena saphena, Applied Mechanics and Materials, 2014, 486: 249-254.

[127] Lin D H S and Yin F C P, A multiaxial constitutive law for mammalian left ventricular myocardium in steady-state barium contracture or tetanus, Journal of Biomechanical Engineering, 1998, 120: 504-517.

[128] McGilvray K C, Sarkar R, Nguyen K and Puttlitz C M, A biomechanical analysis of venous tissue in its normal and post-phlebitic conditions, Journal of Biomechanics, 2010, 43: 2941-2947.

[129] Zulliger M A, Firdez P, Stergiopulos N and Hayashi K, A strain energy function for arteries accounting for wall composition and structure, Journal of Biomechanics, 2004, 37: 989-1000.

[130] Herrera B, Fortuny G and Marimon F, Calculation of human femoral vein wall parameters in vivo form clinical data for specific patient, Journal of Biomechanical Engineering, 2012, 134: 124501-1-4.

[131] Cacho F, Doblare M and Holzapfel G A, A procedure to simulate coronary artery bypass graft surgery, Medical Biological Engineering and Computing, 2007, 45(9): 819-827.

[132] Provenzano P P, Heisey D, Hyashi K, Lakes R and Vanderby R, Subfailure damage in ligament: a structure and cellular evaluation, Journal of Applied Physiology, 2002, 92: 362-371.

[133] Wentzel J J, Kloet J, Andhyiswara I, Oomen J A F, Schuurbiers J C H, de Smet B J G L, Post M J, de Kleijn D, Pasterkamp G, Borst C, Slager C J and Krams R, Shear-stress and wall-stress regulation of vascular remodelling after balloon angioplasty, Circulation, 2001, 104: 91-96.

[134] Gusic R J, Myung R, Petko M, Gaynor J W and Gooch K J, Shear-stress and pressure modulate saphenous vein remodelling ex vivo, Journal of Biomechanics, 2005, 38: 1760-1769.

[135] Tran-Son-Tay R, Hwang M K, Garbey M, Jiang Z H, Ozaki C K and Berceli S A, An experiment-based model of vein graft remodelling induced by shear stress, Annals of Biomedical Engineering, 2008, 36(7); 1083-1091.

[136] Hwang M K, Garbey M, Kim N H and Tran-Son-Tay R, The dynamics of vein graft remodeling induced by hemodynamic forces: a mathematical, Biomechanics Modeling and Mechanobiology, 2012, 11: 411-423.

[137] Hayashi K, Mori K and Miyazaki H, Biomechanical response of femoral vein to chronic elevation of blood pressure in rabbits, American Journal of Physiology Heart Circulation Physiology, 2003, 284: H511-H518.

[138] Kritharis E P, Kakisis, J D, Athina T G, Themistoklis M, Nikos S, Sokrates T and Sokolis, D P, Biomechanical, morphological and zero-stress state characterization of jugular vein remodeling in arteriovenous fistulas for hemodialysis, Biorheology, 2010, 47(5-6): 297-319.

[139] Sassani S G, Theofani A, Tsangaris S, Sokolis D P, Time-course of venous wall biomechanical adaptation in pressure and flow-overload: assessment by a microstructure-based material model, Journal of Biomechanics 2013, 46(14): 2451-2462.

[140] Gomez A D, Zou H S, Shiu Y T and Hsu E W, Characterization of regional deformation and material properties of the intact explanted vein by micro CT and computational analysis, Cardiovascular Engineering and Technology, 2014, 5(4): 359-370.

Table 1 Volume fractions of collagen and elastin in various vascular veins

Vessel	Collagen		Elastin	
	Total	Media	Total	Media
Aorta *	71.4±3.6 $#	52.7±14.7	7.8±3.5 $	8.6±3.5 $
Carotid $	44.7±19.5 *#	39.7±22.4	17.3±5.4 *%#	17.1±6.6 *%
Iliac %	61.6±11.9 #	49.3±16.0	9.6±2.8 $	8.8±3.1 $
Vena cava #	79.7±6.2 *$	32.9±15.4	8.0±2.9 $	8.4±6.4

Volume fractions are presented as percent dry weight, and symbols to the right of the listed volume fraction identify the vessel volume fractions that are significant different (n=5), there are no significant differences in medial collagen across the groups. The table is from [17].

Table 2 Area fractions of collagen, elastin and smooth muscle in various blood vessels of the rabbit

Vessel	Collagen (%)	Elastin (%)	Smooth muscle (%)
Thoracic aorta	28.66	23.58	41.87
Carotid artery	44.11	12.80	34.76
Inferior vena cava	61.99	18.50	8.13
Jugular vein	69.11	5.08	15.45

Area fractions are taken from Fig. 6(c) in [25].

Table 3 Area fractions of collagen and elastin in various vascular veins

Vessel	Collagen		Elastin (%)	Elastin/Collagen index (%)
	Collage I (%)	Collagen IV (%)		
FV	18.0	37.5	9.5	15.0
CSV	35.0	17.5	17.5	24.0
ISV	55.0	15.0	42.5	40.0

Area fractions of transverse section of collagen and elastin in human veins are presented as percent area, FV-femoral vein, CSV-competent saphenous vein, ISV-incompetent saphenous vein. The table drafted is based on Figs 2, 3 to 5 in [29].

Table 4 Existing methods for biomechanical property modelling of venous walls

Type	Method/model	Contributor	Feature
Phenomenological	Uncoupled model	Akio, Masamitsu & Toshiaki (1988) [90]	1) One stress component is fitted by an exponential function of the strain along the stress component direction only; 2) Two stress components are uncoupled.
	Piecewise model	Sokolis (2008) [25]	1) Stress component is fitted by a piecewise expression of power and exponential functions of the strain in the stress component direction.
	Bedspring model	Desch & Weizsacker (2007) [120]	1) Empirical correlation of circumferential-to-longitudinal first Piola-Kirchoff stress ratio in terms of circumferential stretch by hyperbola based on experiment; 2) Longitudinal stretch consists of two parts, one part is related to circumferential stretch only, one part corresponds to longitudinal stress; 3) Longitudinal stress is as a hyperbolic function of the modified longitudinal stretch in which the stretch relating to the circumferential stretch has been excluded.
Strain energy function (deterministic)	Two families of fibres model	Holzapfel, Gasser and Ogden (2000) [97]	1) Axis-symmetrical or diagonal two families of collagen fibres with equal property constants; 2) Fibre orientation without dispersion; 3) Fibre mechanical response as exponential function of squared fibre stretch; 4) Elastin, smooth muscle and the rest material form homogenous matrix, which obeys neo-Hookean model.
	Two families of fibres with different property	Alastrue, Pena, Martinez & Doblare (2008) [122]	1) Axis-symmetrical two families of fibres with different property constants; 2) Fibre orientation without dispersion; 3) Fibre mechanical response as parabolic function of squared fibre stretch; 4) Elastin, smooth muscle and the rest material form homogenous matrix, which obey neo-Hookean model.
	Two families of fibres with orientation dispersion	Gasser, Ogden and Holzapfel (2006) [123]	1) Axis-symmetrical two families of fibres with equal property constants; 2) Fibre orientation with dispersion; 3) Fibre mechanical response as exponential function of squared fibre stretch; 4) Elastin, smooth muscle and the rest material form homogenous matrix, which obeys neo-Hookean model.
	Four families of fibres model	Sokolis (2013) [98]	1) Four families of fibres (two diagonal with equal property constants, one circumferential and one longitudinal with their own constant); 2) Fibre orientation without dispersion; 3) Fibre mechanical response as exponential function of squared fibre stretch; 4) Elastin, smooth muscle and the rest material form homogenous matrix, which yields neo-Hookean or quadratic model.

Table 4 Existing methods for biomechanical property modelling of venous walls (continued)

Type	Method/model	Contributor	Feature
Strain energy function (stochastic)	Two families of fibres with anisotropic elastin and fibre recruitment	Rezakhaniha and Stergiopulos (2008) [124]	1) Axis-symmetrical two families of fibres with the same property constants; 2) Fibre orientation without dispersion; 3) Individual fibre mechanical response obeys a recruitment law, the total fibre response is the integral of all individual fibre contributions. 4) Elastin is homogenous but with isotropic and anisotropic parts, the isotropic part yields modified neo-Hookean model, while the anisotropic part obeys a new strain energy function.
	Two families of fibres with anisotropic elastin, fibre orientation dispersion and fibre recruitment	Agianniotis, Rezakhaniha & Stergiopulos (2011) [125]	1) Axis-symmetrical two families of fibres with the same property constants; 2) Fibre orientation with dispersion; 3) Individual fibre mechanical response obeys a recruitment law, the total fibre response is the integral of all individual fibre contributions. 4) Elastin is homogenous but with isotropic and anisotropic parts, the isotropic part yields modified neo-Hookean model, while the anisotropic part obeys a new strain energy function.

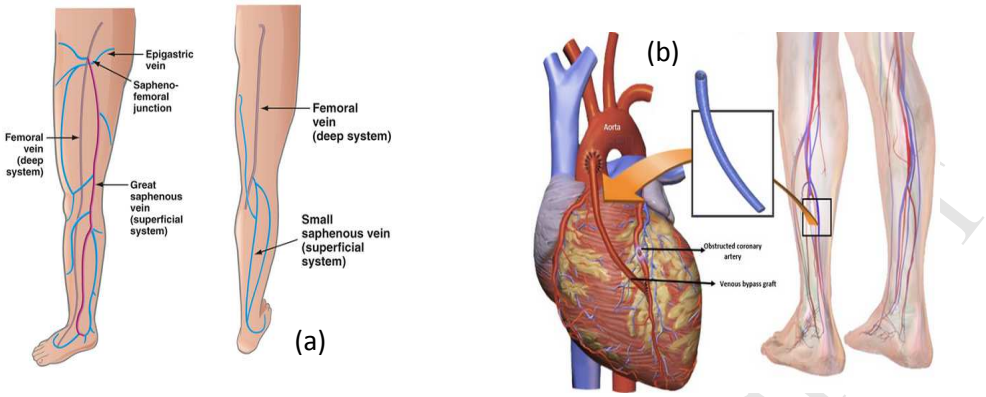

Fig. 1 Greater saphenous vein in human leg (a) and its bypass graft (b), the picture (a) was from [4], the picture (b) was on [5]

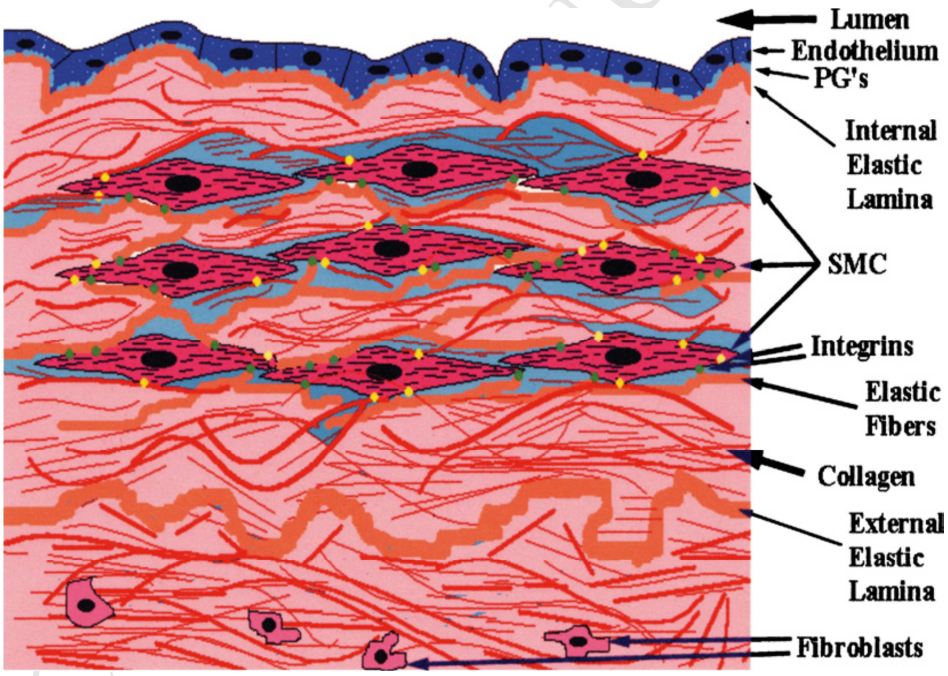

Fig. 2 Image of the transverse section in a vascular wall. In the picture, large fusiform cells are smooth muscel cell (SMC), elastic tissue (thick fibres) and collagen (thin wavy fibres) are connected to integrins on the SMC surface (dots on cell perimeter) and the fibres are oriented in the circumferential direction. Proteoglycans (PG, lightly shaded) surround the SMC. There are links between collagen and elastin fibres. Endothelial cells (cuboidal) also have some PGs connected with them. Fibroblasts (small irregular cells) occur in the adventitia, which is composed mostly of collagenous tissue. This picture is from [17].

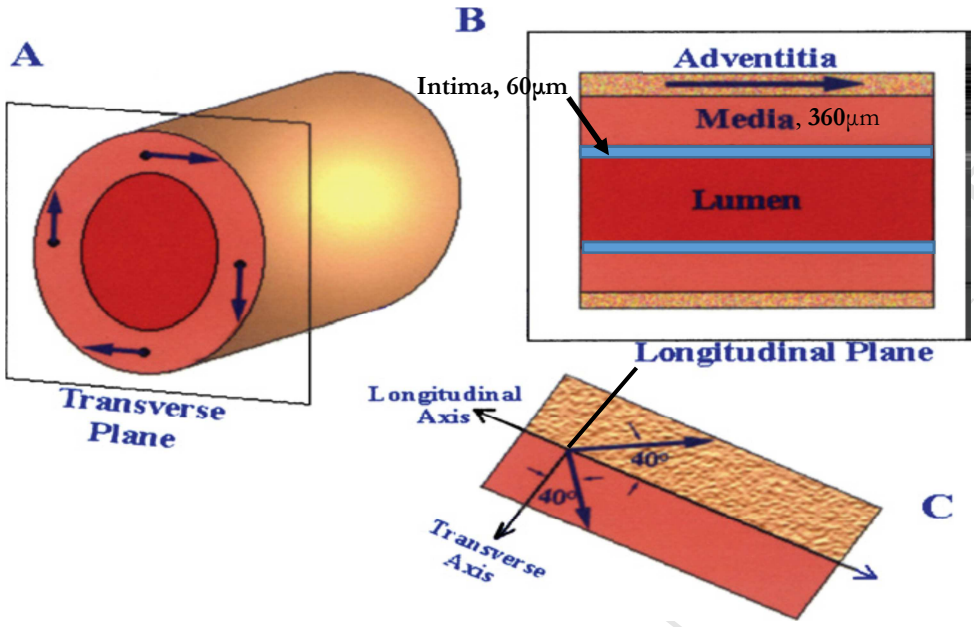

Fig. 3 Histology and mean fibre orientation of porcine vascular tissues the picture was from [17]

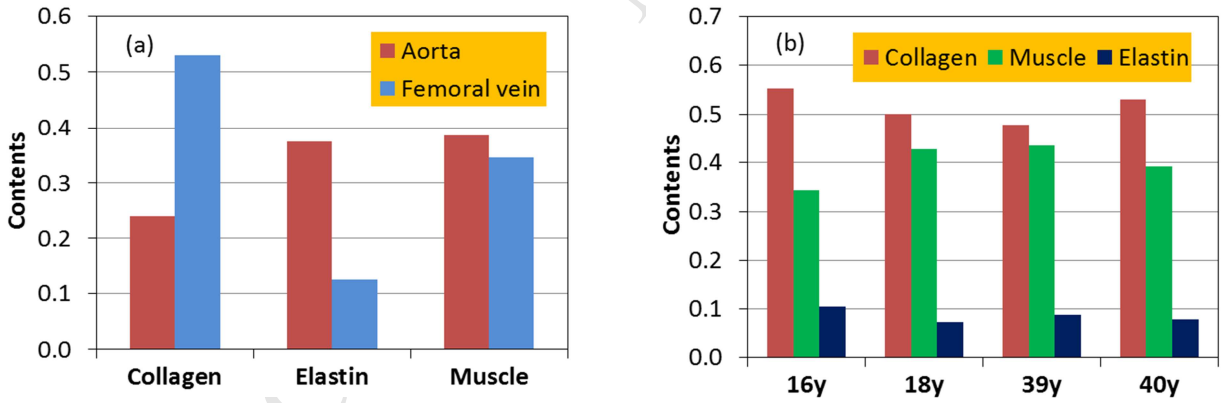

Fig. 4 Dry weigh contents of collagen, elastin and smooth muscle in walls of man aorta, femoral vein and super segments of saphenous vein, (a) aorta and femoral vein(mean of six observation [28]), (b) saphenous vein of subjects in various ages (mean for the veins in the left and right legs [28])

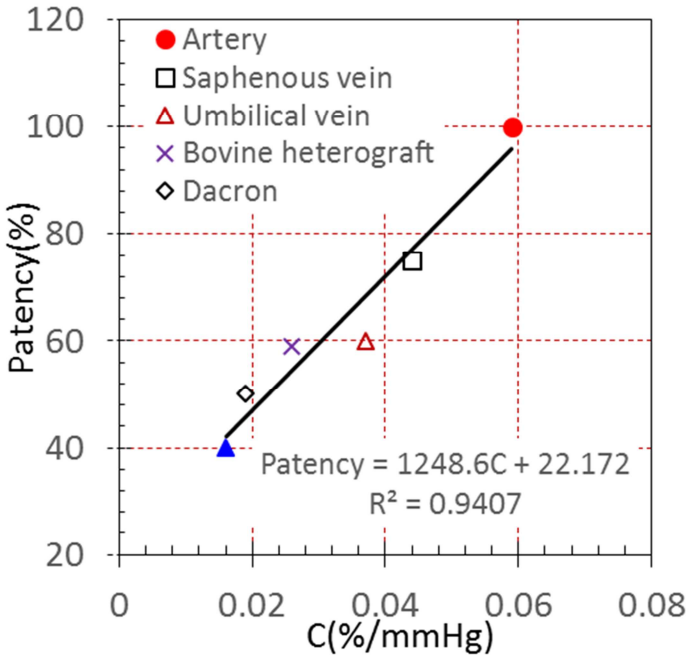

Fig. 5 Relationship between patency and compliance one year after graft surgery

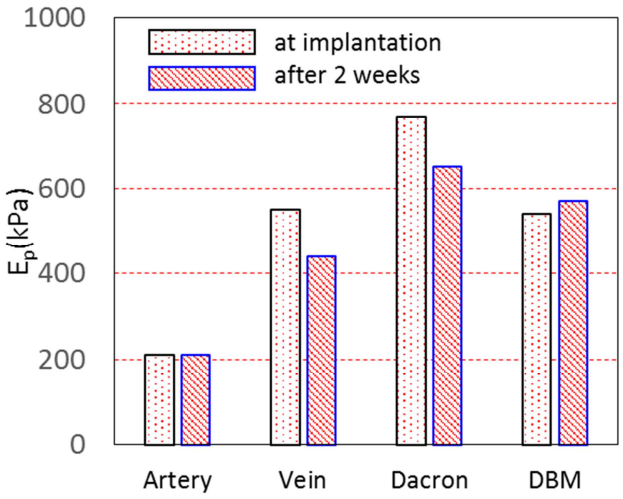

Fig. 6 Changes in global Young's moduli at graft implantation and after 2weeks

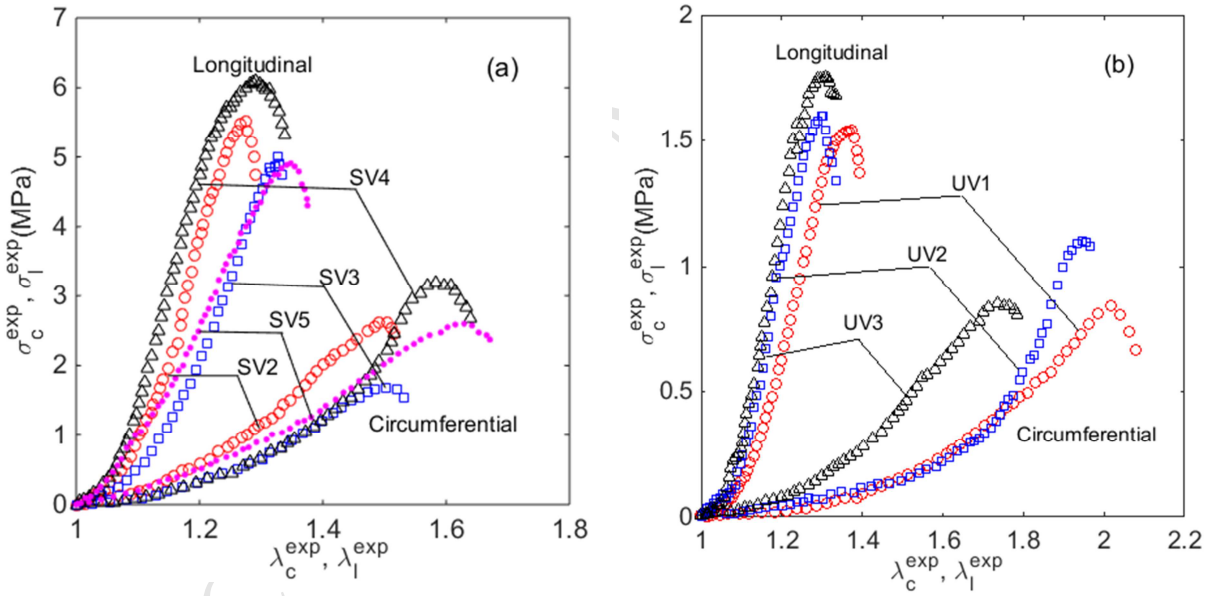

Fig. 7 Experimental stress-stretch data of human saphenous and umbilical veins in [64], (a) saphenous veins (SV), SV2-SV5, (b) umbilical veins(UV), UV1-UV3

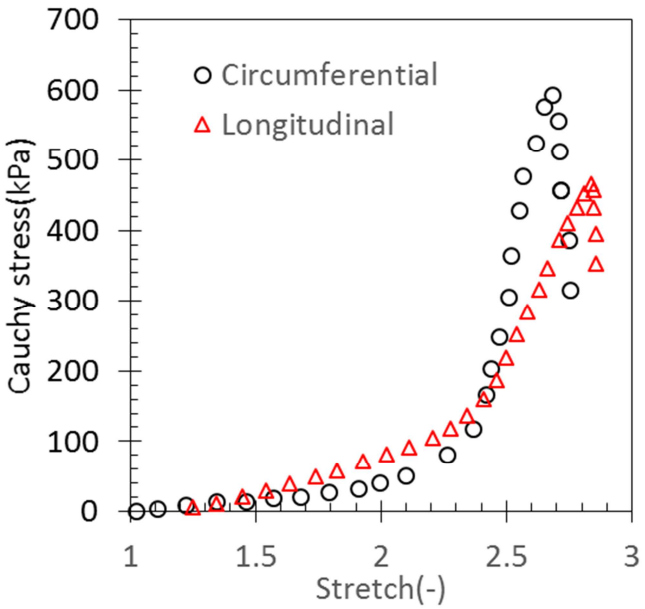

Fig. 8 Cauchy stress-stretch data of bovine vein tested in [92], strain rate is 100%/s

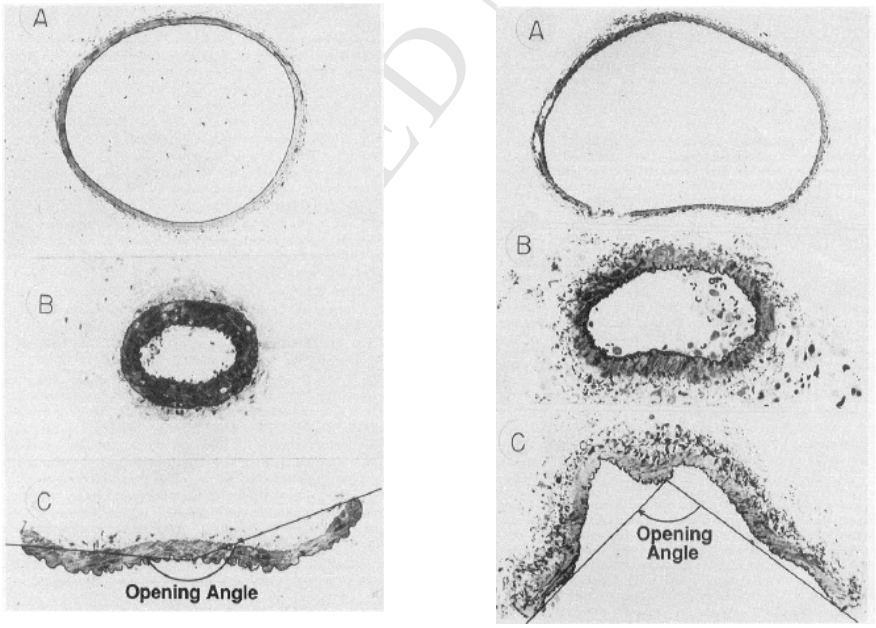

Fig. 9 Opening angle definition, the left: ileal artery fixed at three states: 120mmHg blood pressure (A), zero load (B) and zero stress (C), the right: ileal vein fixed at three states: 3mmHg blood pressure (A), zero load (B) and zero stress (C), the pictures are from [111]

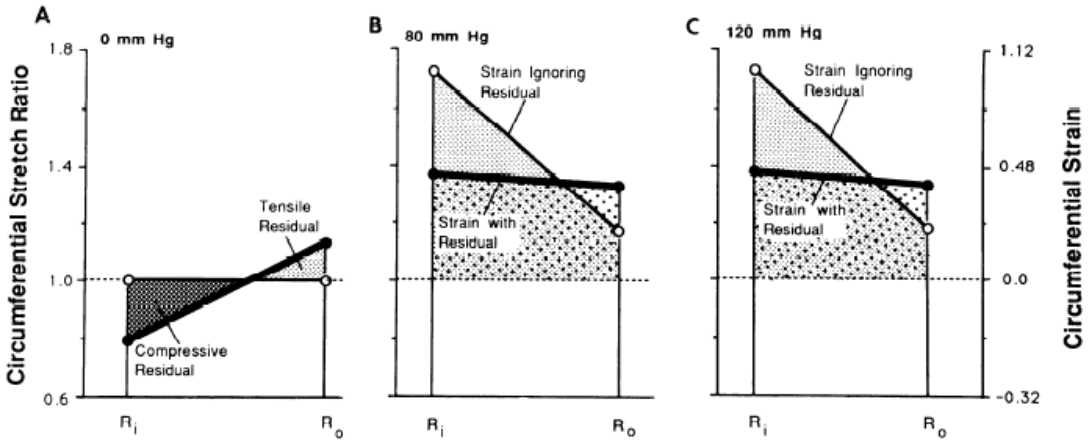

Fig. 10 Circumferential stress distribution across the ileal arterial wall. Zero load (A), 80 mmHg blood pressure (B) and 120mmHg blood pressure (C), the pictures are from [111]

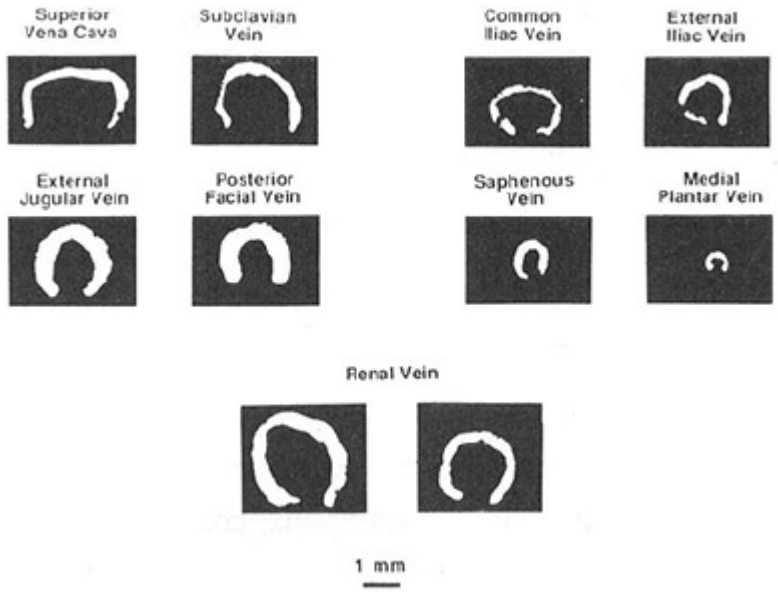

Fig. 11 Typical zero stress states of rat veins, the pictures are after [115]

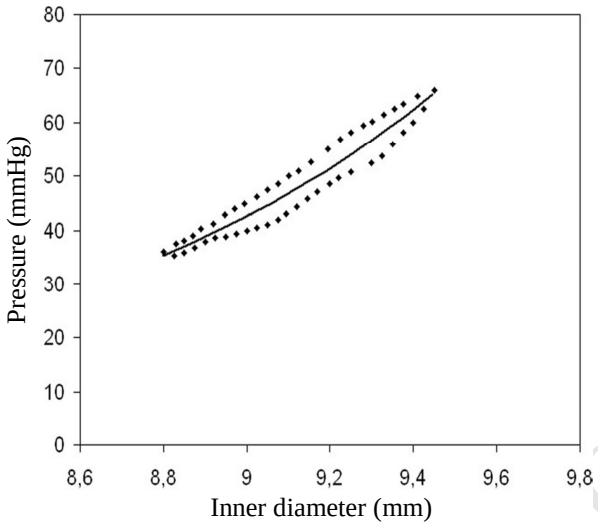

Fig. 12 Comparison of inner diameter of vein between observation and prediction, the picture is after [130]

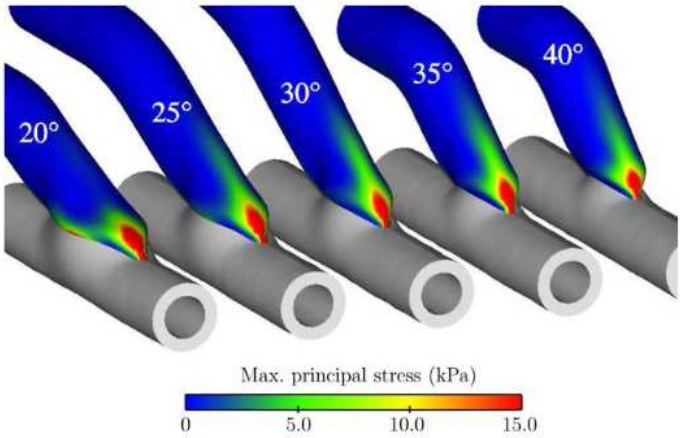

Fig. 13 The first principal stress contour in the implanted Saphenous vein grafts at various insertion angles, the picture is after [131]

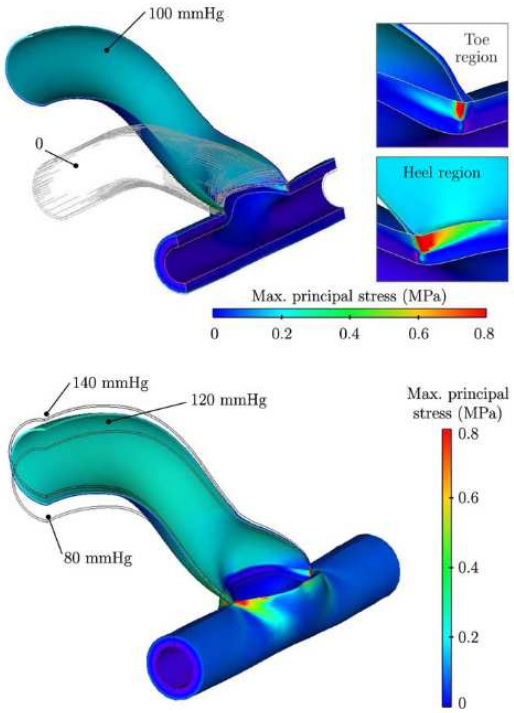

Fig. 14 The first principal stress contour and saphenous vein deformation at 0, 80, 100, 120 and 140mmHg arterial mean pressure, the insertion angle is 25°, the picture is after [131]

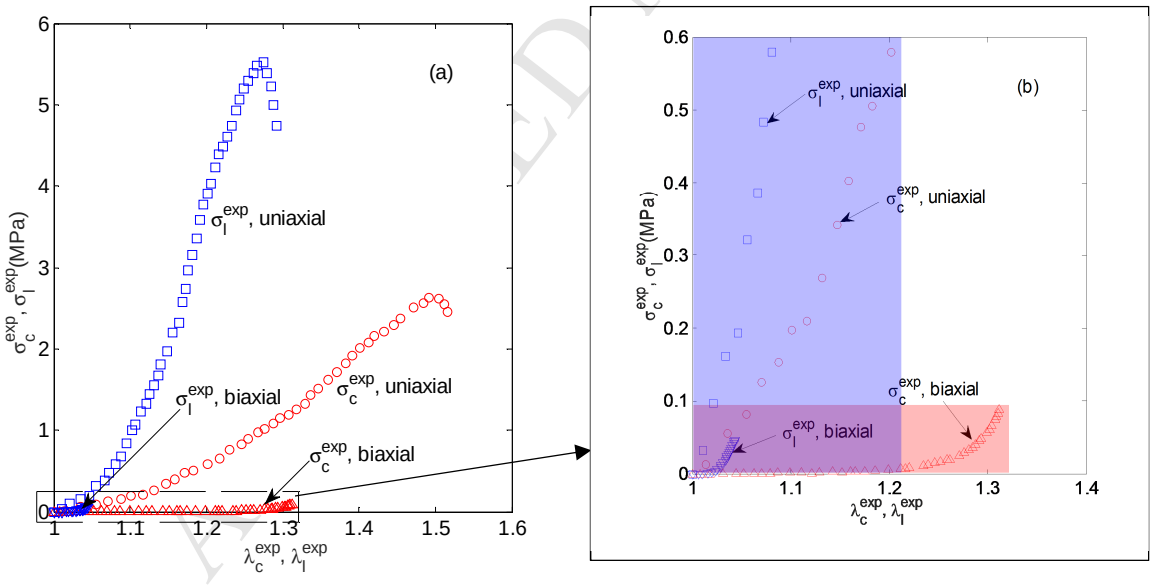

Fig. 15 A comparison of Cauchy-stretch curves measured by uniaxial and tubular biaxial tensile tests, the tensile test data of sample saphenous vein 2 (SV2) are from [64], the first tubular biaxial inflation test data are from [99] at 4Hz loading rate on the human saphenous vein segment

Highlights:

- Biomechanical properties and modelling methods of the human venous wall are critical for coronary artery bypass graft.
- Active and passive biomechanical behaviours of the human venous wall were reviewed extensively and comprehensively.
- Biomechanical properties of the human venous wall are not well documented.
- Modelling approaches are subjected to be updated significantly.
- Important issues, namely suitability of constitutive law, biomechanical property identification in vivo, tissue damage effect etc. should be addressed in the future.